

**Dissertation**

submitted to the

Combined Faculties for the Natural Sciences and for Mathematics  
of the Ruperto-Carola University of Heidelberg, Germany

for the degree of

Doctor of Natural Sciences

presented by

Diplom: Yongjoon Suh

born in: Kangwondo, South Korea

Oral-examination: 12<sup>th</sup> Feb. 2009

Differential Effect of DLX2 in Neural Precursors Derived  
from the Anterior and Hippocampal Subventricular zone

**Referees**

**Prof. Dr. Hilmar Bading**

**Prof. Dr. Gabriele Elisabeth Pollerberg**

# Table of Contents

List of Figures	7
Summary	9
Zusammenfassung	10
Articles from this PhD thesis	11
<b>1. Introduction</b>	<b>12</b>
1.1. Neurogenesis	12
1.2. Neural stem cells during embryonic development	13
1.3. Neural stem cells in the adult brain	16
1.4. Neurogenic regions in the postnatal brain	17
1.5. Regional specification and migration of neural precursors during embryonic development	21
1.6. Distal-less homeobox-2 (DLX2)	25
1.7. The Aims of the Work	28
<b>2. Materials and Methods</b>	<b>29</b>
<b>2.1. Materials</b>	<b>29</b>
2.1.1. General reagents	29
2.1.2. Plasmids	30
2.1.3. Oligonucleotides	30
2.1.4. Enzymes	31
2.1.5. Quantitative PCR reagents	32
2.1.6. Mouse and cell lines	32

2.1.7. Cell culture reagents and media	32
2.1.8. Antibodies	34
2.1.8.1. Primary antibodies	34
2.1.8.2. Secondary antibodies	34
<b>2.2. Methods</b>	<b>35</b>
<b>2.2.1. Methods in Nucleic Acids</b>	<b>35</b>
2.2.1.1. Purification of Nucleic Acids	35
2.2.1.1.1. Mini-preparation	35
2.2.1.1.2. Maxi-preparation	35
2.2.1.1.3. Extraction of DNA from agarose	35
2.2.1.1.4. PCR product purification	36
2.2.1.1.5. RNA extraction	36
2.2.1.2. Photometric determination of DNA and RNA concentrations	36
2.2.1.3. Restriction of DNA	37
2.2.1.4. Ligation of DNA	37
2.2.1.5. Agarose gel electrophoresis of DNA	38
2.2.1.6. Transformation of <i>E. coli</i>	38
2.2.1.7. Polymerase Chain Reaction (PCR)	39
2.2.1.8. Semi-quantitative RT PCR	40
2.2.1.9. Quantitative RT-PCR	42
2.2.1.10. Gateway cloning	42
2.2.1.10.1. BP reaction	43
2.2.1.10.2. LR reaction	43
2.2.1.11. Lentiviral plasmid construction	44

2.2.1.11.1. Amplification of <i>Dlx2</i> gene	44
2.2.1.11.2. Cloning of <i>Dlx2</i> into lentiviral plasmid	45
<b>2.2.2. Methods in Proteins</b>	<b>48</b>
2.2.2.1. Cell lysis for protein	48
2.2.2.2. SDS PAGE	49
2.2.2.3. Western Blot	50
<b>2.2.3. Lentiviral production and transduction</b>	<b>51</b>
<b>2.2.4. Tissue dissection</b>	<b>52</b>
<b>2.2.5. Cell culture</b>	<b>54</b>
2.2.5.1. Bacterial cell culture	54
2.2.5.2. HEK293FT cell culture	55
2.2.5.2.1. Cell line and culture conditions	55
2.2.5.2.2. Freezing and thawing cells	55
2.2.5.2.3. Transfection	56
2.2.5.3. Primary neural precursor cell (NPC) culture	57
<b>2.2.6. Clonal analysis</b>	<b>58</b>
<b>2.2.7. Fluorescence Activated Cell Sorting (FACS)</b>	<b>59</b>
<b>2.2.8. Immunocytochemistry</b>	<b>60</b>
<b>3. Results</b>	<b>62</b>
<b>3.1. Comparative analysis of EGFR<sup>high</sup> cells isolated from the two main neurogenic regions</b>	<b>62</b>
3.1.1. Isolation and clonal analysis of EGFR <sup>high</sup> cells	62
3.1.2. Localization of clone-forming cells within the hippocampus	65
3.1.3. Origin of hippocampal EGFR <sup>high</sup> cells	67

3.1.4. Differential expression of genes associated with transit-amplifying cells between EGFR <sup>high</sup> cells isolated from the GE and the hippocampus	68
<b>3.2. Lentivirus-mediated <i>Dlx2</i> gene delivery and expression</b>	<b>70</b>
<b>3.3. Effect of DLX2 over-expression on hippocampal and aSVZ NPCs</b>	<b>74</b>
3.3.1. DLX2 increases cell proliferation rate	74
3.3.2. Effect of DLX2 over-expression on the differentiation of hippocampal and aSVZ NPCs	76
3.3.3. Effect of DLX2 over-expression on clone formation	79
<b>3.4. Mechanisms underlying the effect of DLX2 over-expression on clone formation</b>	<b>81</b>
3.4.1. The effect of DLX2 on proliferation depends on EGFR signaling	81
3.4.2. DLX2 over-expression increases the number of EGFR <sup>high</sup> cells in cultures of aSVZ but not hippocampal NPCs	82
3.4.3. DLX2 over-expression promotes the transition from EGFR <sup>low</sup> to EGFR <sup>high</sup> clone-forming cells in aSVZ but not hippocampal NPCs	84
3.4.4. EGFR transcription is not regulated by DLX2	86
<b>4. Discussion</b>	<b>88</b>
4.1. Hippocampal EGFR <sup>high</sup> cells display intrinsically different properties from aSVZ EGFR <sup>high</sup> cells	88
4.2. Relationship between precursors in the hSVZ and neurogenesis in the dentate gyrus	90
4.3. Differential effect of DLX2 in precursors of the aSVZ and the hippocampus	92

<b>5. Conclusions and prospects</b>	<b>95</b>
<b>6. References</b>	<b>97</b>
<b>7. Abbreviations</b>	<b>104</b>
<b>8. Acknowledgements</b>	<b>106</b>

## List of Figures

Figure 1.1. Defining properties of neural stem cells	13
Figure 1.2. Two types of NPCs during embryonic development	15
Figure 1.3. Lineage of neural stem cells (blue) during CNS development	17
Figure 1.4. Structure and cytoarchitecture of the postnatal aSVZ	19
Figure 1.5. Structure and cytoarchitecture of the subgranular zone (SGZ)	21
Figure 1.6. Homeobox genes and regional specification of neural precursors in mouse embryonic forebrain	23
Figure 1.7. Expression domains of <i>Dlx</i> genes during mouse embryonic brain development	27
Figure 2.1. Amplification of <i>Dlx2</i> cDNA by RT-PCR	45
Figure 2.2. Cloning of lentiviral constructs	47
Figure 3.1. Clonal analysis of EGFR <sup>high</sup> cells derived from the aSVZ and the hippocampus	64
Figure 3.2. Clonogenic cells in the hippocampus at postnatal day 7 are mostly localized in the hippocampal subventricular zone (hSVZ)	66
Figure 3.3. Expression of <i>Nkx2.1</i> in hippocampal EGFR <sup>high</sup> cells	67

Figure 3.4. Quantitative analysis of <i>Egfr</i> and <i>Dlx2</i> mRNA levels in E18 EGFR <sup>high</sup> cells sorted by FACS	69
Figure 3.5. Analysis of lentiviral-mediated gene delivery and expression	73
Figure 3.6. Effect of DLX2 on clone size	75
Figure 3.7. DLX2 promotes neuronal differentiation	77
Figure 3.8. Quantitative analysis of the percentage of plated cells undergoing secondary clone formation	78
Figure 3.9. Effect of DLX2 over-expression on the percentage of clone-forming cells present in cultures of aSVZ and hippocampal NPCs	80
Figure 3.10. Effect of DLX2 on proliferation depends on EGFR signaling	82
Figure 3.11. Effect of DLX2 on the number of EGFR <sup>high</sup> cells	84
Figure 3.12. Effect of DLX2 on cell lineage transition	86
Figure 3.13. DLX2 does not affect levels of EGFR mRNA	87
Figure 4.1. Schematic model of DLX2 effect in NPCs derived from the aSVZ and the hippocampus	95

## Summary

In the anterior subventricular zone (aSVZ) of the postnatal murine brain, quiescent neural stem cells (NSCs) divide rarely to generate transit-amplifying precursors (TAPs) expressing high levels of epidermal growth factor receptor (EGFR) and distal homeobox (DLX)-2 transcription factor. Both NSCs and TAPs form clones upon EGF stimulation. Similar cells expressing high levels of EGFR (EGFR<sup>high</sup>) are also present in the hippocampus. However, it is not clear whether they represent NSCs and whether they undergo a lineage progression similar to aSVZ precursors. In this study, clonogenic EGFR<sup>high</sup> cells were isolated from the postnatal (or prenatal) mouse aSVZ (or GE) and hippocampus by flow cytometry. I found that *Nkx2.1*, a regional marker of medial ganglionic eminence (MGE), is also expressed in hippocampal EGFR<sup>high</sup> cells as well as GE precursors, indicating that at least a subset of hippocampal clonogenic EGFR<sup>high</sup> precursors originates from the MGE during embryonic development. Microdissection of the hippocampus following FACS and clonal analysis revealed those clonogenic cells are localized to the hippocampal SVZ (hSVZ), rather than the dentate gyrus (DG), neurogenic region in the hippocampus. However, hippocampal EGFR<sup>high</sup> cells expressed less *Egfr* and *Dlx2* mRNA, than GE EGFR<sup>high</sup> cells. Reflecting the differential pattern of gene expression, clonal analysis revealed hippocampal EGFR<sup>high</sup> cells are less self-renewing and proliferative than EGFR<sup>high</sup> cells derived from the aSVZ. Forced expression of DLX2 increased the proliferative and neurogenic capacity of aSVZ clone-forming precursors by promoting neuroblast generation. DLX2 over-expression also increased the ability of aSVZ stem cells to form clones in response to EGF by promoting a lineage transition from NSCs to TAPs. Finally, over-expression of DLX2

in hippocampal precursors had a similar effect on neurogenesis but not on NSC lineage progression. Taken together, these observations suggest that clonogenic EGFR<sup>high</sup> cells in the hSVZ originate from the GE; however, they are intrinsically different from aSVZ precursors with respect to their stem cell properties.

## Zusammenfassung

Im postnatalen Mäusegehirn befinden sich neurale Stammzellen (NSCs) in der anterioren subventrikulären Zone (aSVZ). NSCs teilen sich nur selten und generieren bei ihrer Zellteilung schnell proliferierende Vorläuferzellen (transit-amplifying precursors; TAPs). TAPs exprimieren den Homeobox-Transkriptionsfaktor Distalles-2 (DLX2) und weisen eine starke Expression des Rezeptors des Epidermalen Wachstumsfaktors (EGFR<sup>high</sup> Zellen) auf. Nach Stimulation mit exogenem EGF *in vitro* bilden TAPs, wie auch NSCs der SVZ, Klone. Auch einige Zellen des Hippocampus zeigen ein hohes Expressionsniveau des EGFR. Ob diese Zellen NSCs repräsentieren und eine ähnliche Abfolge an Vorläuferzellen bilden wie NSCs der aSVZ ist jedoch noch ungeklärt. In der vorliegenden Arbeit wurden aus dem Gehirn pre- und postnataler Mäuse EGFR<sup>high</sup> Vorläuferzellen des Striatums (ganglionic eminence, GE) beziehungsweise der aSVZ und des Hippocampus mit Hilfe eines Durchflußzytometers isoliert. Dabei konnte gezeigt werden, dass *Nkx2.1*, ein Marker für Zellen der medialen GE (MGE), auch in EGFR<sup>high</sup> Zellen des Hippocampus exprimiert wird. Dies deutet daraufhin, dass zumindest eine Subpopulation der hippocampalen EGFR<sup>high</sup> Vorläuferzellen während der Embryonalentwicklung von der MGE abstammen.

Separate Analysen von EGFR<sup>high</sup> Zellen der hippocampalen SVZ and des Gyrus Dentatus (dentate gyrus; DG) hinsichtlich ihrer Fähigkeit, Klone zu generieren, zeigte, dass solche klonbildende Zellen vorwiegend in der hippocampalen SVZ und nicht im DG lokalisiert sind. Diese hippocampalen EGFR<sup>high</sup> Zellen exprimieren die mRNA des *Egfr* und des Transkriptionsfaktors *Dlx2* auf einem niedrigerem Niveau als EGFR<sup>high</sup> Zellen der GE. Dieses Ergebnis spiegelt sich auch in dem verminderten Potenzial dieser Zellen zur Selbsterneuerung und zur Proliferation im Vergleich zu EGFR<sup>high</sup> Vorläuferzellen der aSVZ wieder. Überexpression von DLX2 verstärkt hingegen das proliferative und neurogene Potenzial klonbildender Vorläuferzellen der aSVZ durch Förderung der Neuroblastenbildung. Des Weiteren beschleunigt die Überexpression von DLX2 den Übergang von NSCs zu TAPs und somit die Fähigkeit von Stammzellen der aSVZ in Gegenwart von EGF Klone zu bilden. Die Überexpression von DLX2 in hippocampalen Vorläuferzellen zeigt zudem ähnliche Effekte auf die Neurogenese, aber nicht auf die Bildung von TAPs aus NSCs. Diese Beobachtungen weisen darauf hin, dass klonbildende EGFR<sup>high</sup> Zellen in der hippocampalen SVZ von der GE abstammen, aber intrinsische Unterschiede bezüglich ihrer Stammzeleigenschaften von anterioren SVZ Stamm- und Vorläuferzellen aufweisen.

## Articles from this PhD thesis

### **Analysis of the effect of DLX2 in neural precursors of the anterior and hippocampal subventricular zone reveals intrinsic differences between these two cell populations**

Yongjoon Suh, Carmen Carrillo-García, Kirsten Obernier, Gabi Hölzl-Wenig, Kerstin Horsch, Volker Eckstein and Francesca Ciccolini. To be submitted to Stem Cells

# 1. Introduction

## 1.1. Neurogenesis

Neurogenesis, a process of generating new neurons from neural stem/precursor cells (NPCs) was traditionally believed to occur only during embryonic stages in the mammalian central nervous system. However, it is now established that NPCs are also present in the adult mammalian brain. Furthermore, cell-tracing studies have confirmed that neurogenesis continues in restricted areas of the brain throughout the lifespan of the animal.

NPCs have been defined on the basis of their potential to generate multiple cell types (e.g. neurons, astrocytes and oligodendrocytes) and their ability to self-renew *in vitro* (Fig 1.1). During development, NPCs progressively modify their morphological and antigenic characteristics as well as their potential to generate different progenitor types (Merkle FT 2006). Thus, this introduction will start to describe how NPCs are specified in space and time, and change their appearance.

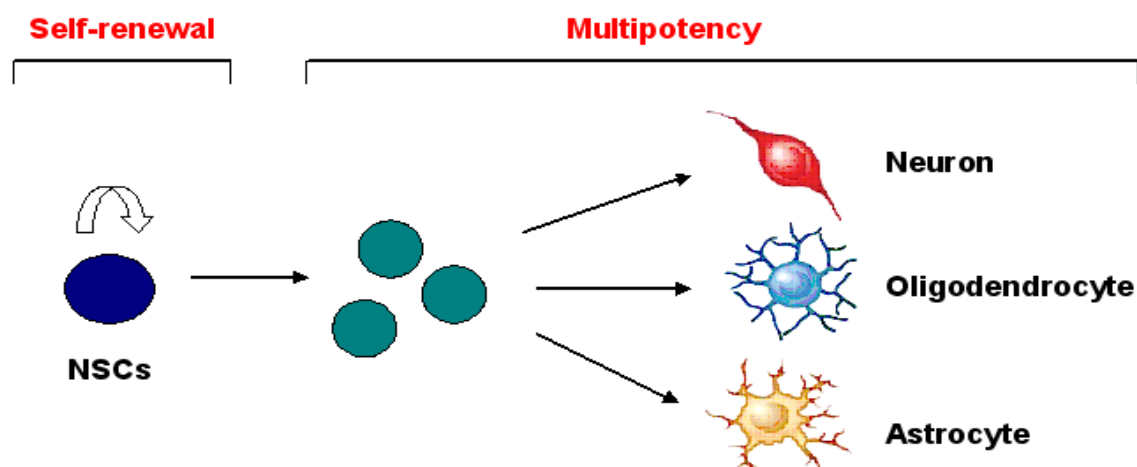


**Fig 1.1. Defining properties of neural stem cells**

Neural stem cells can give rise to more stem cells (self-renewal) and give rise to neurons, astrocytes and oligodendrocytes (multipotency).

## 1.2. Neural stem cells during embryonic development

The central nervous system (CNS) is originally formed by the neural plate, a layer of NPCs named as neuroepithelial cells. The lateral edges of this sheet fold together to form the neural tube, whose fluid-filled cavity will subsequently give rise to the ventricular system and spinal canal. Neuroepithelial cells are radially elongated and contact both the apical (ventricular) and basal (pial) surfaces. Radial glia, a second NPC type appears before the beginning of neurogenesis. Since radial glia and neuroepithelial cells share many characteristics, including the maintenance of some features of apical-basal polarity and the expression of the intermediate filament protein nestin (Alvarez-Buylla A 2001), it is thought that neuroepithelial cells transform directly into radial glial cells stretching to maintain contact with both the apical and basal brain surface while

the thickness of the brain increases during development (Fig 1.2A). However, this transformation has not yet been experimentally demonstrated.

Radial glia cells were originally thought to have a mere structural function and considered a scaffold for neuronal migration. However, they have now been shown to function as neural stem cells that give rise to glia and neurons *in vitro* and *in vivo* (Malatesta P 2000; Merkle FT 2004; Malatesta P 2008). In the ventricular zone, radial glia cells undergo either symmetric division to generate two radial glial cells, or divide asymmetrically. By asymmetric divisions radial glia precursors will give rise to a new radial glial cell and either a neuron, which migrates into the cortical plate through the intermediate zone, or a basal progenitor, which moves to the subventricular zone (SVZ) and divides symmetrically to generate two neurons (Fig 1.2B).

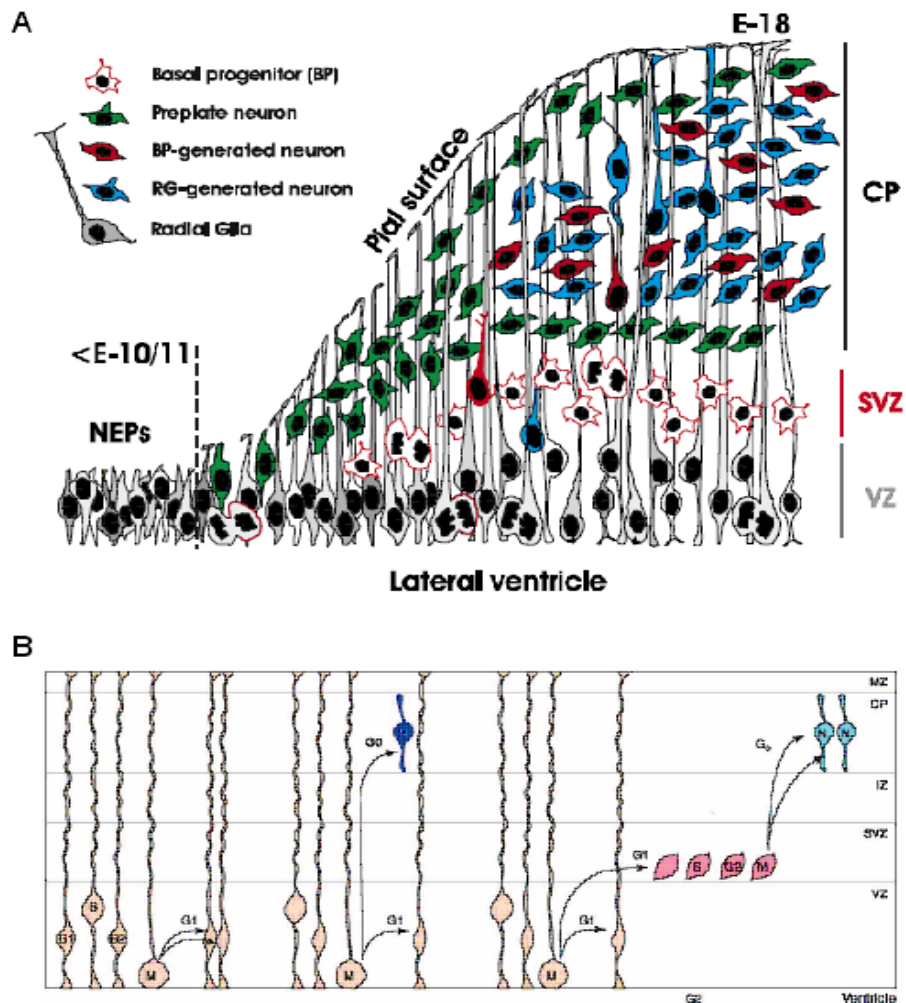


### Fig 1.2. Two types of NPCs during embryonic development

(A) During forebrain development, neuroepithelial cells progressively convert to radial glia that elongate following the thickening of the neural tube wall. Neurons (green and red) are generated from basal progenitors which are generated from neuroepithelial at early stages or radial glia at later stages. Neurons (blue) are also generated directly from radial glia at later stages. (Figure adapted from (Malatesta P 2008)). (B) Radial glia cells divide in the ventricle zone either symmetrically to generate two radial glial cells, or asymmetrically to generate a radial glial cell and either a neuron, which migrates away from the germinal region to more superficial layers, or a basal progenitor, which divide symmetrically to generate two neurons. NEPs, neuroepithelial precursors; CP, cortical plate; IZ, intermediate zone; MZ, marginal zone; CP, cortical plate; SVZ, subventricular zone; VZ, ventricular zone. This cartoon has been adapted from (Guillemot F 2005).

### **1.3. Neural stem cells in the adult brain**

Radial glial cells share many features with astrocytes of the anterior SVZ (aSVZ) in postnatal mouse brain. Both cell types reside in the germinal epithelium at different developmental times, and some aSVZ astrocytes maintain a polarized morphology with a long radial process similar to that of radial glia. In songbirds and other organisms, a subset of radial glia remains neurogenic during adult life (Alvarez-Buylla A 1990; Garcia-Verdugo JM 2002; Russo RE 2004; Zupanc GK 2006). In mammals, this function appears to be carried out instead by the germinal zone astrocytes, which are direct descendants of radial glia. Experiments with a Cre-lox-based strategy to specifically label neonatal radial glia have shown that these cells give rise to multiple cell types, including the astrocytes of the aSVZ (Merkle FT 2004). Therefore, it has been proposed that adult neural stem cells are part of a continuous lineage from neuroepithelial cells to astrocytes in the adult germinal zone, with radial glia representing the intermediate precursor type (Fig. 1.3).

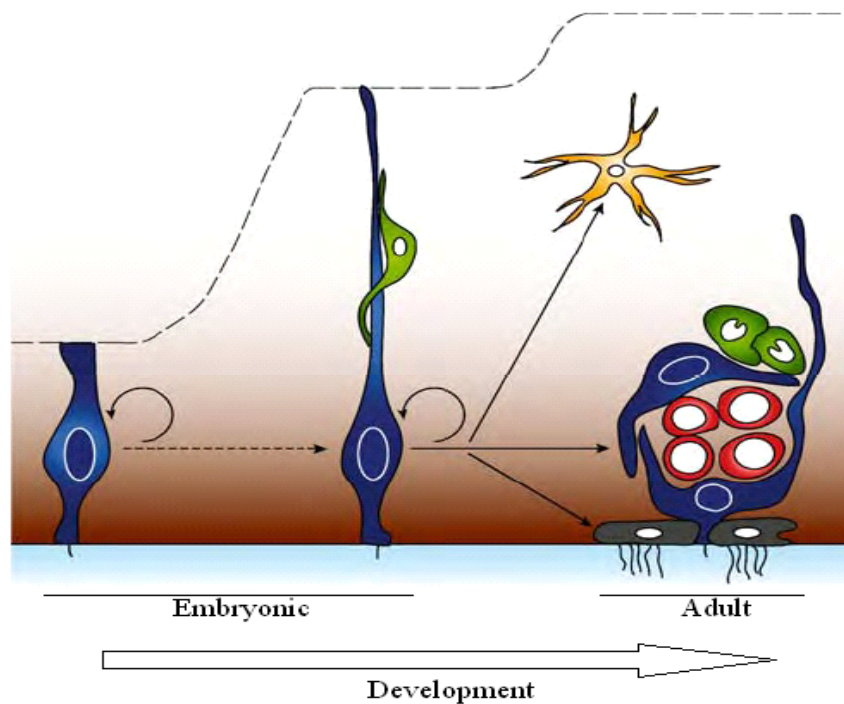


### Fig 1.3. Lineage of neural stem cells (blue) during CNS development

NPCs change their shape and produce distinct progeny as the brain develops. Neuroepithelial cells are the principle neural stem cells of the early developing brain. During brain development, these cells may change to radial glia, which in turn gives rise to the astrocyte-like neural stem cells in the postnatal aSVZ. Both neuroepithelial cells and radial glia maintain contacts with both the ventral surface and pial surface of the brain and project a single cilium into the developing ventricle. Although aSVZ astrocytes does not contact the pial surface, they often project a single cilium to the ventricle. This cartoon has been adapted from (Ihrie RA 2008) and modified.

### 1.4. Neurogenic regions in the postnatal brain

In the adult brain, generation of new neurons occurs throughout life primarily in two specific regions; the aSVZ of lateral ventricle and the subgranular zone (SGZ) of hippocampal dentate gyrus (DG) (Temple S 1999; Gage FH 2000).

In the aSVZ, three main types of precursors drive the process of neurogenesis leading to the generation of olfactory inhibitory interneurons throughout adulthood (Fig 1.4) (Alvarez-Buylla A 2004). Primary NPCs, known as type B, exhibit structural and biological markers of astrocytes. Type B cells undergo rare cell divisions and generate rapidly dividing precursors, called type C cells, which in turn give rise to immature neuroblasts also termed type A cells (Doetsch F 1997). Newly generated neuroblasts are arranged in tubes of tangentially oriented cells ensheathed by astrocytes. Such chains of neuroblasts form a complicated network throughout the wall of the lateral ventricle, immediately below the ependymal layer which lines the ventricular cavity. Migrating neuroblasts converge in the anterior dorsal SVZ to form the rostral migratory stream (RMS) leading to the olfactory bulb where neuroblasts will differentiate into interneurons. Fundamental elements of the stem cell niche in the postnatal aSVZ are represented by the extracellular matrix, blood vessels and microglia (Fig 1.4) (Mercier F 2002). A subset of type B cells contacts the lateral ventricle via a cilium (Doetsch F 2002) and the blood vessels via an elongated basal process. This highly specialized architecture allows extensive cell-cell interaction and the propagation of signals from the cerebrospinal fluid in the ventricle, the surrounding extracellular matrix and local blood vessels.

Both type B primary precursors and type C cells are able to self-renew in response to growth factors (EGF and FGF-2), forming neurospheres which contain neural stem cells and differentiated NPCs that, upon removal of exogenous growth factors, differentiate to neurons, astrocytes and oligodendrocytes (Doetsch F 2002). Thus, both type B and type C cells are clone-forming cells and multipotent *in vitro*. However, only type B cells express the intermediate filament protein glial fibrillary associated protein (GFAP)

whereas distalless (DLX)2 homeoprotein is found in type C cells and neuroblasts but not in stem cells (Doetsch F 2002). DLX2, as a homeodomain transcription factor, is essential for neuronal differentiation of late born precursors (after embryonic days 12.5) in the basal ganglia and for their migration to the cerebral cortex, olfactory bulb and hippocampus during embryonic development (Anderson SA 1997; Anderson SA 1997; Eisenstat DD 1999). Besides promoting neurogenesis during embryonic development, DLX2 also promotes neurogenesis in the postnatal aSVZ, albeit at this age the function of DLX2 is still unclear (see also below 1.6).

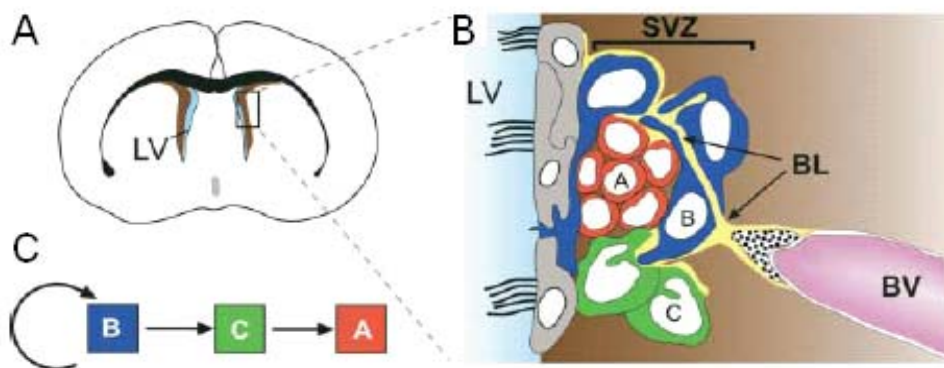


**Fig 1.4. Structure and cytoarchitecture of the postnatal aSVZ**

(A) Schematic illustration of a coronal section of the adult mouse brain. The ventricular area contained in the squared region is magnified in (B). The aSVZ is localized next to walls of the lateral ventricles (LV) and is separated from the ventricular cavity by a layer of ependymal cells. Neuroblasts (type A cells, red) are surrounded by astrocyte-like neural stem cells (type B cells, blue), whereas transit-amplifying cells (type C cells, green) are localized on the side of the neuroblast chain. A subset of type B cells has direct contact with the lateral ventricle (LV) via a short cilium. Type B cells also contact with the basal lamina (BL) surrounding the blood vessels (BV). (C) Lineage relationship between different aSVZ precursor types. Type B cells generate type C cells, which will give rise to type A cells. This cartoon has been adapted from (Alvarez-Buylla A 2004).

The subgranular zone (SGZ) of the dentate gyrus (DG) in the hippocampus is also a major site of adult neurogenesis. In contrast to the aSVZ, the SGZ is not in direct contact with the lateral ventricle and the cerebrospinal fluid (Fig 1.5). Furthermore, cells born in the SGZ migrate a short distance and differentiate into granule neurons in the DG (Cameron HA 1993). As in the aSVZ, primary SGZ precursors are also represented by GFAP+ astrocytes and give rise to granule neurons via generating intermediate progenitor cells (Seri B 2001). In the SGZ, a group of astrocytes have a prominent radial process and extend shorter tangentially oriented processes at the base of the SGZ (Fig 1.5). These cells, called radial astrocytes, have been identified as the primary SGZ neural stem cells (Seri B 2001; Filippov V 2003; Fukuda S 2003; Steiner B 2006). The SGZ also contains horizontally oriented astrocytes that lack a radial process (Fig 1.5). It is not known whether these astrocytes also act as precursor cells.

Unlike stem cells derived from the aSVZ, SGZ precursors do not display stem cell properties such as long-term self-renewal and multipotency *in vitro*. NPCs have also been identified in the hippocampal subependyma (hSVZ) (Seaberg RM 2002; Bull ND 2005). In contrast to SGZ precursors, these cells display *in vitro* properties of stem cells and in the neonatal brain generate cells that migrate to surrounding regions including the SGZ (Navarro-Quiroga I 2006). Thus, although neurogenesis clearly occurs in the SGZ of the hippocampal DG, it remains still controversial whether these cells represent *bona fide* neural stem cells. In the first part of this doctoral work, I further investigated this specific issue by directly isolating hSVZ and SGZ precursors and performing a comparative analysis of their properties.

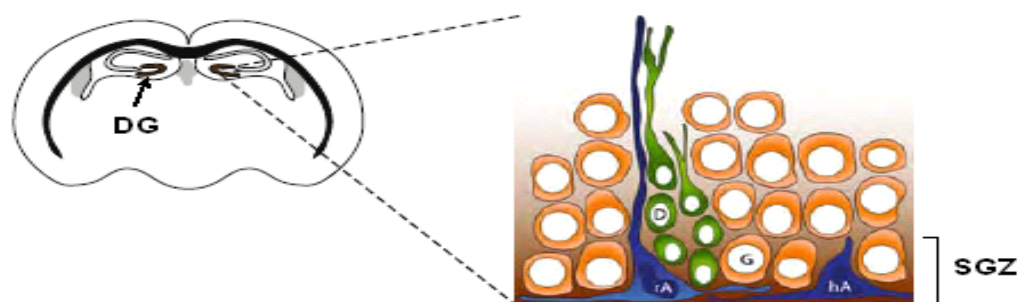


**Fig 1.5. Structure and cytoarchitecture of the subgranular zone (SGZ)**

Schematic illustration of a coronal section of the adult mouse brain shows that the SGZ is located within the dentate gyrus of the hippocampus. The SGZ contain radial (rA) and horizontal (hA) astrocytes. Radial astrocytes have long radial processes that penetrate the granular layer and tangential processes that are oriented parallel to this layer. These astrocytes give rise to type D immature precursors (D), which divide and further differentiate into new granule neurons (G). This cartoon has been adapted from (Ihrig RA 2008) and modified.

**1.5. Regional specification and migration of neural precursors during embryonic development**

During embryonic forebrain development, neural precursors are specified by regional and temporal cues present in the germinative niche. The mechanisms of regional specification of neural precursors in the forebrain remain unclear. However, genetic analyses have revealed that expression of specific transcription factors in a regionally restricted manner is a key to the specification of regional identity within the telencephalon. Through a mechanism that involves mutually repressive interactions, these transcription factors establish boundaries between different precursor zones, leading to the establishment of precursor domains. For example, specification of the medial ganglionic eminence (MGE) and anterior entopeduncular area (AEP) requires

the expression of the homeobox transcription factor *Nkx2.1* (Sussel L 1999) (Fig 1.6). In the absence of *Nkx2.1*, progenitor cells from the MGE and AEP are re-specified to the more dorsal fate, similar to that of lateral ganglionic eminence (LGE) progenitors (Fig 1.6B) (Sussel L 1999). Similarly, the homeodomain gene *Gsh2* is required for the specification of the dorsal part of the LGE. In mice lacking *Gsh2* function, dorsal LGE progenitor cells express molecular markers that are associated with the cortex, indicating that this transcription factor is necessary to establish the boundary between the LGE and the adjacent cortex (Corbin JG 2000; Toresson H 2000; Yun K 2001) (Fig 1.6). *Pax6* and *Nkx2.1* antagonize each other to establish the boundary between the MGE and LGE (Sussel L 1999; Stoykova A 2000). Accordingly, *Pax6* mutants show a phenotype that is complementary to the one displayed by *Nkx2.1* mutants. In *Pax6* mutant mice, LGE precursor cells are re-specified to a more ventral fate, leading to an expansion of the MGE (Fig 1.6B). In addition, *Pax6* and *Gsh2* have opposing roles in the establishment of the boundary between the LGE and cortex (Toresson H 2000; Yun K 2001). So, loss of *Pax6* function results in the expression of dorsal LGE markers in the cortex, and severe disruption of the boundary between the cortex and basal ganglia.

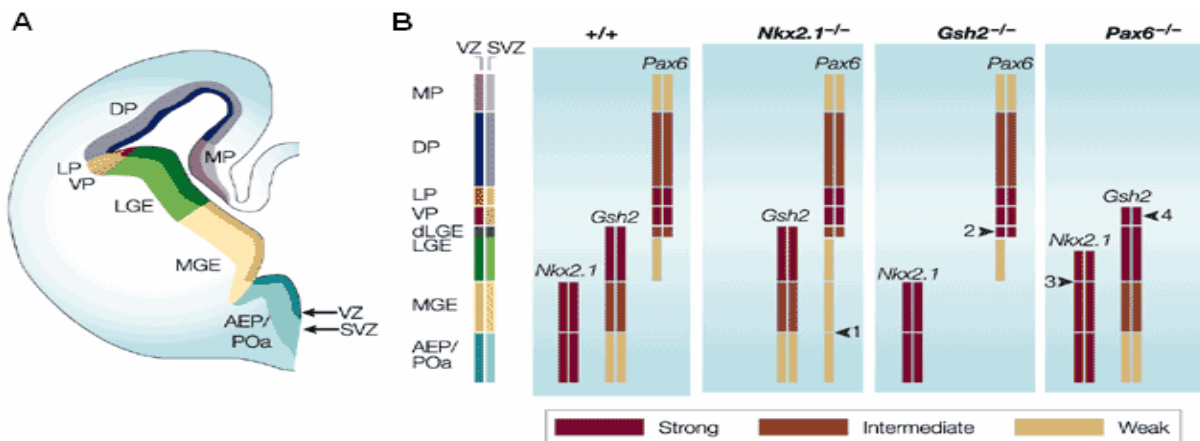


### Fig 1.6. Homeobox genes and regional specification of neural precursors in mouse embryonic forebrain

(A) Schematic drawing of a coronal hemisection through the murine brain at embryonic day 14.5, showing distinct precursor cell domains of the telencephalon. (B) The expression of *Nkx2.1*, *Gsh2* and *Pax6* is required to define independent precursor cell populations in the lateral ganglionic eminence (LGE) and medial ganglionic eminence (MGE). Gene interaction defines boundaries between the different precursor zones. In *Nkx2.1* mutants, *Pax6* expression is expanded ventrally in the MGE and anterior preoptic area (AEP) (arrowhead 1). In *Gsh2* mutants, *Pax6* expression is expanded ventrally into the dorsal LGE (dLGE), along with other pallial markers (arrowhead 2). Finally, in *Pax6* mutants, *Nkx2.1* expression is expanded dorsally into the LGE (arrowhead 3) and *Gsh2* expression is expanded dorsally into the ventral pallium (VP) (arrowhead 4). DP, dorsal pallium; LP, lateral pallium; MP, medial pallium; POA, anterior preoptic area; SVZ, subventricular zone; VZ, ventricular zone. This cartoon has been adapted from (Marin O 2001).

Once neural precursors are specified, they are set to migrate to their final position in the mantle of the forebrain. Regionally specified neural precursors migrate via diverse pathways to reach their final destinations in the developing mammalian telencephalon. Two general modes of migration occur in the embryonic forebrain; radial migration, in which cells migrate from the germinal zone toward the surface of the brain along the

radial glia scaffold; and tangential migration, in which cells migrate orthogonal to the direction of radial migration. Most newborn cortical neurons migrate radially from the ventricular zone to the overlying mantle zone, while some neural precursors migrate tangentially from the basal ganglionic eminence to the cortex, the olfactory bulb and the hippocampus. The routes of tangential migration from the basal telencephalon to the cortex have been studied by means of vital dye labelling (de Carlos JA 1996; Anderson SA 1997; Wichterle H 1999). Further studies have shown that in the murine brain tangentially migrating cells mostly give rise to GABAergic interneurons (Anderson SA 1997; Sussel L 1999; Pleasure SJ 2000; Corbin JG 2001; Marin O 2001).

Mice lacking transcription factor, *Nkx2.1* that is required for the MGE development showed a reduction of GABAergic interneurons in the cortex. Analysis of this mutant strain has indicated that the MGE contributes at least ~50% of GABAergic interneurons to the developing cortex. Besides the cortex, *Nkx2.1* expressing cells also give rise to GABAergic interneurons in the hippocampus (Pleasure SJ 2000). During migration, a subset of cells seems to keep the expression of their regional transcription factor, *Nkx2.1* (Marin O 2000). Mice with mutation of *Dlx1/2* showed more severe reduction of GABAergic neurons in the developing cortex and hippocampus, suggesting many of tangentially migrating cells appear to require the function of the *Dlx2* homeobox gene (Anderson SA 1997; Pleasure SJ 2000; Nery S 2003).

In this doctoral work, therefore, I explored the relationship between hippocampal clone-forming cells and tangentially migrating cells originated from the basal ganglionic eminence by investigating the expression of transcription factors involved in the regional specification of NPCs.

## 1.6. Distal-less homeobox 2 (DLX2)

The *Dlx* genes are the murine orthologs of the *Drosophila* gene *distalless*. The *Dlx* genes encode homeodomain proteins that are required for forebrain and craniofacial development. Of six known mouse *Dlx* genes, four (*Dlx1*, *Dlx2*, *Dlx5* and *Dlx6*) are expressed in the developing CNS (Anderson SA 1997; Liu JK 1997; Eisenstat DD 1999). *Dlx* genes are expressed in the two longitudinal domains described in the prosomeric model of forebrain development (Rubenstein JL 1994). *Dlx1/Dlx2* and *Dlx5/Dlx6* genes are arranged in bigenic clusters on mouse chromosomes 2 and 6 (Zhou QP 2004) and map to human chromosomes 2q31.1 and 7q21.3, respectively. *Dlx1* and *Dlx2* are only 10 kb apart on mouse chromosome 2 near the *HoxD* locus (McGuinness T 1996). The four *Dlx* genes in the forebrain are sequentially expressed (Fig 1.7; *Dlx2* → *Dlx1* → *Dlx5* → *Dlx6*) and have overlapping domains of expression in the subpallium: DLX1 and DLX2 are localized to the ventricular zone, DLX1/2/5 to the SVZ and DLX5/6 to the mantle zone. There are distinct boundaries of DLX1/DLX2 expression at the pallial/subpallial boundary (Fig 1.7).

Mice lacking *Dlx1*, *Dlx2*, *Dlx5*, *Dlx1/Dlx2* and *Dlx5/Dlx6* have been generated and their phenotypes analyzed (Panganiban G 2002). All *Dlx* heterozygote mice are normal. Single *Dlx1* or *Dlx2* homozygous mutants die at birth with relatively subtle forebrain defects (Qiu M 1995). Mice lacking both genes have a time-dependent block in striatal neurogenesis and also die at P0 (Anderson SA 1997). Although *Dlx2* expression starts around embryonic 9.5 (E9.5), only cells born after E12.5 are impaired in their migration and remain in the SVZ. In *Dlx1/Dlx2* double mutants, tangential migration from the MGE to the LGE is also blocked (Anderson SA 1997) and *Dlx1/Dlx2* double mutants

lack GABAergic interneurons in the olfactory bulb and in the hippocampus (Pleasure SJ 2000). After birth, *Dlx2* is expressed in transit amplifying cells and immature neuroblasts of the aSVZ. However, few studies have investigated the function of *Dlx2* in the postnatal brain. In this study I have manipulated the expression of DLX2 in NPCs derived from the aSVZ and the hippocampus. These experiments were aimed at further investigating the function of DLX2 in NPCs and neurogenesis as well as at unveiling intrinsic differences between these two precursor groups.

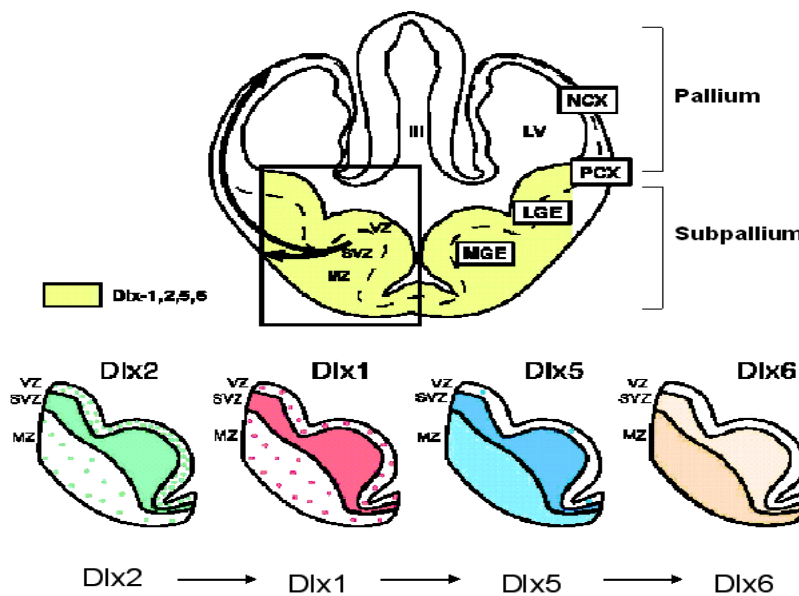


**Fig 1.7. Expression domains of *Dlx* genes during mouse embryonic brain development**

Most cells in the subpallial telencephalon express *Dlx1*, *Dlx2*, *Dlx5* and *Dlx6* at different stages of differentiation. The arrows indicate cell migration from the subpallium to the pallium (cortex). The *Dlx* genes appear to be expressed in sequential manner (*Dlx2*→*Dlx1*→*Dlx5*→*Dlx6*). *Dlx2* is expressed in scattered cells in the VZ and mantle zone (green dots), and in most cells in the SVZ (uniform green). *Dlx6* is primarily expressed in differentiated cells in the mantle zone (uniform peach). *Dlx1* (red) and *Dlx5* (blue) are expressed in intermediate patterns. NCX, neocortex; PCX palliocortex; LGE, lateral ganglionic eminence; MGE, medial ganglionic eminence; VZ, ventricular zone; SVZ, subventricular zone; LV, lateral ventricle; III, third ventricle. This cartoon has been adapted from (Panganiban G 2002) and modified.

### **1.7. The Aims of the work**

Neurogenesis in adult mammalian brain has a great potential to develop new strategies to treat a number of incurable brain disorders, from neurodegenerative disease to brain and spinal cord injuries, multifocal diseases and tumors. To fully realize the potential of neural stem cell therapy, it is necessary to know their identity, the signals and the molecular mechanisms by which their proliferation/differentiation is regulated. Neurogenesis in the aSVZ and in the hippocampus appears to be regulated by different mechanisms and it is not clear whether this is due to intrinsic functional differences between the populations of NPCs residing in these neurogenic regions.

Thus, to investigate this issue I focussed on the following specific aims:

- (1) To isolate and characterize putative neural stem cells in the hippocampus and in the aSVZ
- (2) To investigate expression pattern of specific genes in two groups of NPCs
- (3) To investigate the function of DLX2 in NPCs

## 2. Materials and Methods

### 2.1. Materials

#### 2.1.1. General reagents

<u>Reagents</u>	<u>Company</u>
Agarose	Invitrogen
40% Acrylamide/Bis	Roth
Ammonium persulfate	Roth
Boric acid	J.T Baker
Bromophenolblue	CHROMA
BSA	Roth
Chloroform	Fluka
DAPI	Boehringer
EDTA	Applichem
Enhanced Luminol reagent	PerkinElmer
Ethanol	Sigma
Ethidiumbromide	Serva
Glycine	Sigma
Isopropanol	Applichem
Low melting agarose	Invitrogen
Methanol	Sigma
Moviol	Calbiotech
Non fat milk powder	Frema/Reform

NP-40	CN Biomedicals Inc.
PageRuler Prestained protein ladder	Fermentas
Paraformaldehyde	Fluka
SDS	Serva
Sucrose	Riedel-deHaën
TEMED	Merck
Tria base	Roth
Trizol	Invitrogen
Tween 20	Roth

\* Other general reagents and chemicals like MgCl<sub>2</sub>, CaCl<sub>2</sub>, NaCl etc. were purchased from Sigma

### 2.1.2. Plasmids

pFUGW (Lois C 2002)

pFUGW Dlx2

pLenti6 CITE EGFP (modified pLenti6/V5DEST (Invitrogen) by (Oh-hora M 2003))

pLenti6 CITE EGFP Dlx2

pDlx2 (modified from pEGFP-N1 vector; GenBank Accession #U55762)

pCMVdelta8.9 (Lentiviral packaging plasmid)

pVSVG (pseudotyping plasmid) (Naldini L 1996; Zufferey R 1997)

### 2.1.3. Oligonucleotides

Dlx2 forward primer with BamHI      5` - AGGATCCTCTTTCTGTCCCGGGTCAGG-3`

Dlx2 reverse primer with NheI      5` -TGCTAGCGAAAATCGTCCCCGCGCTC-3`

Dlx2 reverse primer with *NotI* 5'-**AGCGGCCGCTTAGAAAATCGTCCCCGC**-3'

(annealing sequences are underlined, extensions containing restriction sites are shown in bold).

The *attB*-containing *Dlx2* forward primer:

5'-GGGGACAAGTTTGTACAAAAAAGCAGGCTTCAGG**ATGACTGGAGTCTTTGACAGTC**-3'

The *attB*-containing *Dlx2* reverse primer:

5'-GGGGACCACTTTGTACAAGAAAGCTGGGTG**TTAGAAAATCGTCCCCGCGCTCAC**-3'

(*Dlx2* specific sequences are underlined).

Nkx2.1-forward primer	5'-TACAGGTT <b>CAGTCCAGGCTG</b> -3'
Nkx2.1-reverse primer	5'-TGAAAAAGT <b>GAGGGACTAGG</b> -3'
Dlx2-forward primer	5'-GGATGACTGGAGTCTTTGACAGTC-3'
Dlx2-reverse primer	5'-GCTTGTGCAGGCTGCTGTTGCTGC-3'
GFP-forward primer	5'-CCTACGGCGTGCAGTGCTTCAGC-3'
GFP-reverse primer	5'-CGAGCTGCA CGCTGCCGTCCTC-3'
Gapdh-forward primer	5'-ACCACAGTCCATGCCATCAC-3'
Gapdh-reverse primer	5'-TCCACCACCCTGTTGCTGTA-3'

#### 2.1.4. Enzymes

Restriction enzymes	New England Biolabs or MBI Fermentas
T4 DNA Ligase	Promega
DNase	Sigma
GoTaq DNA polymerase	Promega

PWO DNA polymerase	Roche
M-MLV Reverse Transcriptase, RNase H Minus	Promega
Trypsin-EDTA	Gibco
Papain	Sigma
BP clonase	Invitrogen
LR clonase	Invitrogen

### 2.1.5. Quantitative PCR reagents

TaqMan <sup>®</sup> Universal PCR Master Mix (10x)	Applied Biosystems
Probes:	
<i>Dlx2</i> (assay ID: Mm00438427_m1)	Applied Biosystems
<i>Egfr</i> (assay ID: Mm00433023_m1)	Applied Biosystems
<i>B2m</i> (assay ID: Mm00437762_m1)	Applied Biosystems

### 2.1.6. Mouse and cell lines

- Mouse : CD1 (Charles River) albino mice or CB57 BL/6  
     Prenatal embryos at day 18 (E18) or postnatal mice at day 7 (P7)
- HEK293FT: cell line established from primary embryonal human kidney transformed  
     with sheared human adenovirus type 5 DNA (Graham FL 1977).

### 2.1.7. Cell culture reagents and media

B-27	Gibco
DMSO	Sigma
Dulbecco's MEM (4.5 g/l glucose)	Gibco
EGF-conjugated Alexa 488	Molecular probes

EGF-conjugated Alexa 647	Molecular probes
Euromed-N medium	Euroclone
F-12	Invitrogen
FCS	BioWhittaker
Glucose	Sigma
Geneticin	Gibco
Human recombinant EGF	Peptotech
Human recombinant FGF2	Peptotech
Leibovitz medium	Gibco
L-Glutamine	Gibco
Lipofectamine 2000	Invitrogen
Non-Essential Amino Acids (100x)	Gibco
OPTI-MEM I Reduced Serum Medium	Invitrogen
Penicillin/Streptomycin	Gibco
PI (propidium iodide)	Sigma
Sodium pyruvate (100x)	Gibco
Trypan Blue	Sigma
Ovomucoid	Sigma

## 2.1.8. Antibodies

### 2.1.8.1. Primary antibodies

Antibody	Dilution ratio		Company
	Immunocytochemistry	Western blot	
Mouse anti- $\beta$ -tubulin type III (Tuj1)	1:400		Sigma
Rabbit anti-Dlx2	1:500	1:800	Chemicon
Rabbit anti-GFP	1:500	1:1000	Molecular Probes
Goat anti-DCX	1:500		Santa Cruz
Mouse anti-alpha Tubulin		1:100000	Sigma

### 2.1.8.2. Secondary antibodies

Antibody	Dilution ratio		Company
	Immunocytochemistry	Western blot	
Anti-rabbit cy3	1:200		Jackson ImmunoRes
anti-mouse alexa 488	1:1000		Molecular Probes
anti-sheep cy3	1:500		Dianova
Goat Anti-Mouse IgG (H+L)		1:5000	Jackson ImmunoRes
Goat Anti-Rabbit IgG (H+L)		1:5000	Jackson ImmunoRes

## **2.2. Methods**

### **2.2.1. Methods in Nucleic Acids**

#### **2.2.1.1. Purification of Nucleic Acids**

##### **2.2.1.1.1. Mini-preparation**

A single bacterial colony was picked with a sterile tip and was inoculated to 3 ml of LB medium containing appropriate antibiotics. Plasmid was isolated from 2 ml of overnight cell culture. The purification procedure was performed using QIAprep Spin Miniprep kit (Qiagen) according to the manufacturer's instructions.

##### **2.2.1.1.2. Maxi-preparation**

A single bacterial colony was picked with a sterile tip and was inoculated to 200 ml of LB medium containing appropriate antibiotics. Plasmid was isolated from 200 ml of overnight cell culture. The purification procedure was performed using HiPure plasmid Maxiprep kit (Invitrogen) according to the manufacturer's instructions.

##### **2.2.1.1.3. Extraction of DNA from agarose**

DNA fragments were purified by QIAquick Gel Extraction Kit (Qiagen). The procedures were followed as indicated in the protocol of the manufacturer. Finally, DNA fragments were eluted with 30  $\mu$ l Elution buffer.

### **2.2.1.1.4. PCR product purification**

To change buffer condition for enzymatic reactions such as restriction or ligation, PCR-amplified DNA fragment was purified by Qiaquick PCR Purification kit (Qigen).

### **2.2.1.1.5. RNA extraction**

Cells in Trizol (1~1.5 ml) were briefly homogenized by pipetting. Chloroform was added as 0.33 times as the volume of Trizol and strongly vortexed for 15 sec. All the above procedures were done at room temperature. After vortexing, it was centrifuged at 4 °C for 15 min. The upper phase was taken to a new tube and the isopropanol was added approximately 0.5 volumes of Trizol. It was incubated at least 10 min at room temperature and centrifuged at 4 °C. The supernatant was discarded and the pellet was washed with 75% ethanol in RNase-free H<sub>2</sub>O. The ethanol was evaporated at room temperature and then the RNA pellet was suspended in RNase-free H<sub>2</sub>O.

Alternatively, RNA was also extracted by RNeasy Mini Kit (Qiagen). In case of small number of cells (e.g sorted cells), RNA was extracted by RNeasy Micro Kit (Qiagen). For RNA extraction, cells (1000~2000 cells) were directly sorted to lysis buffer (Buffer RLT with beta-mercaptoethanol) and strongly vortexed. All procedures were followed by manufacturer's instructions.

### **2.2.1.2. Photometric determination of DNA and RNA concentrations**

The DNA and RNA concentrations are measured at wavelength 260 nm and calculated by the following formulas:

double stranded DNA : 1 O.D at 260 nm = 50 µg/mL

single stranded RNA : 1 O.D at 260 nm = 40 µg/mL

The purity of DNA or RNA was estimated by the following values:

Pure DNA: A260/A280 ≥ 1.8

Pure RNA: A260/A280 ≥ 2.0

### **2.2.1.3. Restriction of DNA**

For cloning procedure, 5~10 µg of plasmid DNA was restricted in 20~40 µl reaction volume. For restriction analysis, 300~600 ng of plasmid DNA was digested in 15 µl. Around 2 unit of restriction enzyme was used for 1 µg DNA plasmid digestion. The reaction was done at 37 °C for 2 hours.

### **2.2.1.4. Ligation of DNA**

Ligation reaction was prepared in 14 µl volume and incubated at room temperature for 1 hour. Approximately 150 ng DNA plasmid was used for reaction. The amount of insert DNA fragment was 1:3 molar ratio of vector:insert and calculated by the following equation.

$$(\text{ng of vector}) \times \frac{\text{kb size of insert}}{\text{kb size of vector}} \times (\text{molar ratio of insert/vector}) = \text{ng of insert}$$

### 2.2.1.5. Agarose gel electrophoresis of DNA

After DNA restriction or PCR reaction, DNA fragments were resolved by size using agarose gel electrophoresis in TBE-buffer. The DNA bands were visible in agarose gel containing ethidium bromide when exposed to UV light. As size marker for DNA, GeneRuler™ 100 bp Plus or  $\phi$ 174 (*Hae* III) or  $\lambda$  DNA (*Hind* III and *Eco*R I) were used. All size markers were purchased from Fermentas.

<b>TBE (10x)</b>	108 g	Tris Base
	55 g	Boric acid
	0.5 M	EDTA 20 ml
	H <sub>2</sub> O filled up to 1000ml	

### 2.2.1.6. Transformation of *E. coli*

Transformation of *E. coli* was carried out using the method of Himeno and coworkers (Himeno 1984). The frozen competent cells were thawed on ice. 100  $\mu$ l of thawed cells was added into a tube containing 14  $\mu$ l of ligation mixture, mixed gently and incubated on ice for 30 min. The tube was then heated at 42 °C thermo block for 1 min. The tube was rapidly transferred and cooled on ice. 1ml of LB medium was added and the cells were incubated at 37 °C for 1hour with agitating. After 1hour, cells were plated on LB agar plates containing antibiotics for selection and were incubated at 37 °C over night.

### 2.2.1.7. Polymerase Chain Reaction (PCR)

PCR reaction was done in 25 or 30  $\mu$ l volume. Pipetting scheme for reaction mixture was prepared as indicated in Table 2.1.

Table 2.1. Pipetting scheme for reaction mixture

Template DNA	1~2 $\mu$ l
Primer (forward)	10~20 pmol
Primer (reverse)	10~20 pmol
dNTP's (10 mM)	0.5 $\mu$ l (or 0.75 $\mu$ l)
Buffer (10x)	2.5 $\mu$ l (or 3 $\mu$ l)
MgCl <sub>2</sub> (25 mM)	0~4 $\mu$ l
Polymerase	0.3 $\mu$ l (1.5 U)
H <sub>2</sub> O	up to 25 $\mu$ l (or 30 $\mu$ l)

Reaction condition was set up depending on primers and amplified DNA fragment size. The annealing condition (temperature and time) was decided by considering length and GC content of primers. The elongation time was set by considering DNA fragment size (~1 min for 1 kb) to be amplified. The amplification cycles usually were 25 to 40 cycles.

Step 1. Denaturing, 2~3 min at 94 °C

Step 2. Denaturing, 30 sec at 94 °C

Step 3. Annealing, 20~40 sec at 55~67 °C

Step 4. Elongation, 20~60 sec at 72 °C (cycle to step 2)

Step 5. 30~40 cycling (2-3-4)

Step 6. Elongation, 3 min at 72 °C

Step 7. Holding at 4 °C

### **Reagents for PCR reaction**

GoTaq DNA polymerase (5 U/μl, Promega)

Green GoTaq Reaction Buffer (5x, Promega)

PWO DNA polymerase (used for *Dlx2* cloning, Roche)

PCR buffer (10x, Roche)

dNTPs (100 mM, Sigma)

MgCl<sub>2</sub> (50 mM, Sigma)

### **2.2.1.8. Semi-quantitative RT PCR**

Total RNA was extracted from cells by RNeasy Mini Kit (Qiagen) according to manufacturer's instructions. 1~2 μg total RNA was reversely transcribed to the first-strand cDNA using oligo dT primers (Promega) by M-MLV Reverse Transcriptase, RNase H Minus (Promega). The mixture 1 (RNA and oligo dT primer in RNase free H<sub>2</sub>O; below Table 2.2) was preheated for 3 min at 80 °C and then cool down on ice. It followed to add mixture 2 (buffer, dNTPs, RNasein, DTT, M-MLV; below Table 2.2). RT reaction was allowed at 42 °C for 50 min. M-MLV was then inactivated at 80 °C for 10 min and reaction mixture was hold on 4 °C. The first-strand cDNA was then amplified with 25 cycles by PCR. The amount of amplified DNA bands was analyzed

by the intensity of ethidium bromide-staining. *Gapdh* was amplified for endogenous control gene.

Table 2.2. Pipetting scheme for reaction mixture

Mixture 1	Mixture 2
1 µg RNA	3 µl Buffer (5x)
0.5 µl Oligo dT primers (0.5 µg /µl)	0.75 µl dNTPs (10 mM)
	0.35 µl RNasin (40 U/µl)
	1.5 µl DTT (100 mM)
	1 µl M-MLV (200 U/µl)
Up to 6 µl RNase free H <sub>2</sub> O	Up to 9 µl RNase free H <sub>2</sub> O

### Reagents for RT reaction

Oligo dT Primers (0.5 µg/ µl, Promega)

dNTPs (10 mM, Promega)

Ribonuclease inhibitor (40 U/µl, Promega)

M-MLV Reverse Transcriptase, RNase H Minus (200 U/ µl, Promega)

Buffer (5x, Promega)

DTT (100 mM, Sigma)

RNase free H<sub>2</sub>O (Qiagen)

### **2.2.1.9. Quantitative RT-PCR**

Cells (2000~3000 cells) were sorted directly into lysis buffer (100 µl) and vortexed strongly. The total RNA was then extracted from cells by RNeasy Micro Kit (Qiagen). Total RNA was reversely transcribed into cDNA using M-MLV reverse transcriptase (Promega) at 42 °C for 50 min in 20 µl reaction volumes. M-MLV was then heat-inactivated at 80 °C for 10 min.

TaqMan gene expression assays for genes of interest, *Dlx2* (assay ID: Mm00438427\_m1), *Egfr* (assay ID: Mm00433023\_m1) and a house-keeping gene, *beta-2 microglobulin (B2m)* (assay ID: Mm00437762\_m1) were purchased from Applied Biosystems. The quantitative reverse transcription (qRT)-PCR was performed in 7300 Real Time PCR system from Applied Biosystems. Ct values (cycle threshold) were obtained from the logarithmic phase of the amplification plot between normalized fluorescence of Fam reporter dye of TaqMan MGB probe and cycle numbers for the PCR. Ct values for *Dlx2* and *Egfr* were normalized against *B2m*.

### **2.2.1.10. Gateway Cloning**

Gateway Cloning is a universal cloning technique developed by Invitrogen life technologies. Gateway Cloning Technique allows transfer of DNA fragments between different cloning vectors while maintaining the reading frame. It has effectively replaced the use of restriction endonucleases and ligases. Using Gateway, one can clone/sub-clone DNA segment for functional analysis. The Gateway Technology is based on the bacteriophage lambda site-specific recombination system which facilitates the integration of lambda into the *E. coli* chromosome and the switch between the lytic

and lysogenic pathways (Ptashne M 1992). In the Gateway Technology, the components of the lambda recombination system are modified to improve the specificity and efficiency of the system (Bushman W 1985). Two recombination reactions constitute the basis of the Gateway cloning.

### **2.2.1.10.1. BP reaction** (PCR fragment + Donor vector = Entry Clone)

BP Reaction facilitates recombination of an *attB* substrate (*attB*-PCR product or a linearized *attB* expression clone) with an *attP* substrate (donor vector) to create an *attL*-containing entry clone. PCR amplified *attB*-containing Dlx2 (20~50 fmol) and donor vector, pDONR221 (150 ng/μl) were mixed in total volume 8 μl TE buffer. Reaction was allowed by adding 2 μl of the BP Clonase™ II enzyme (Invitrogen), gently mixing and incubating at 25°C for 1 hour. Reaction was stopped by adding 1 μl of the Proteinase K solution and incubating at 37°C for 10 min. For one transformation of competent *E. coli*, 1 μl of the BP recombination reaction was used. BP recombination reaction could be stored at -20°C for up to 1 week before transformation, if desired.

### **2.2.1.10.2. LR reaction** (Entry Clone + Destination Vector = Expression Clone)

LR Reaction facilitates recombination of an *attL* substrate (entry clone) with an *attR* substrate (destination vector) to create an *attB*-containing expression clone. This reaction is catalyzed by LR Clonase™ II enzyme mix. Entry vector (pDONR221 Dlx2) and destination vector (pLenti6 CiteEGFP) were mixed in total volume 8 μl TE buffer. Reaction was allowed by adding 2 μl of the LR Clonase™ II enzyme (Invitrogen), gently mixing and incubating at 25°C for 1 hour. Reaction was stopped by adding 1 μl of the Proteinase K solution and incubating at 37°C for 10 min. For one transformation

of competent *E. coli*, 1  $\mu$ l of the LR recombination reaction was used. LR recombination reaction could be stored at -20°C for up to 1 week before transformation, if desired.

### **2.2.1.11. Lentiviral plasmid construction**

#### **2.2.1.11.1. Amplification of *Dlx2* gene**

By PCR, the murine *Dlx2* cDNA (Accession number, NM\_010054) was amplified from the cDNA obtained by reverse transcription of total RNA extracted from neurosphere culture. Due to GC-rich in sequence of *Dlx2* gene, reverse transcription reaction was done at high temperature, 67 °C using C. therm. Polymerase One step RT-PCR system (Roche) to overcome secondary or tertiary structure of GC rich template, and was amplified by PCR using PWO DNA polymerase (Roche) with proof reading activity. Also, two parts of *Dlx2* gene was amplified by each PCR reaction. At first PCR, two parts of *Dlx2* gene fragment (501 bp and 558 bp) was amplified by each set of primers as shown in Fig 2.1A and B. At 2<sup>nd</sup> PCR, a full length of *Dlx2* (1031 bp) was amplified (Fig 2.1A and C). For cloning sites, two restriction sites (*Bam*HI and *Nhe*I) were introduced at each ends of *Dlx2* gene and stop codon was deleted by primers.

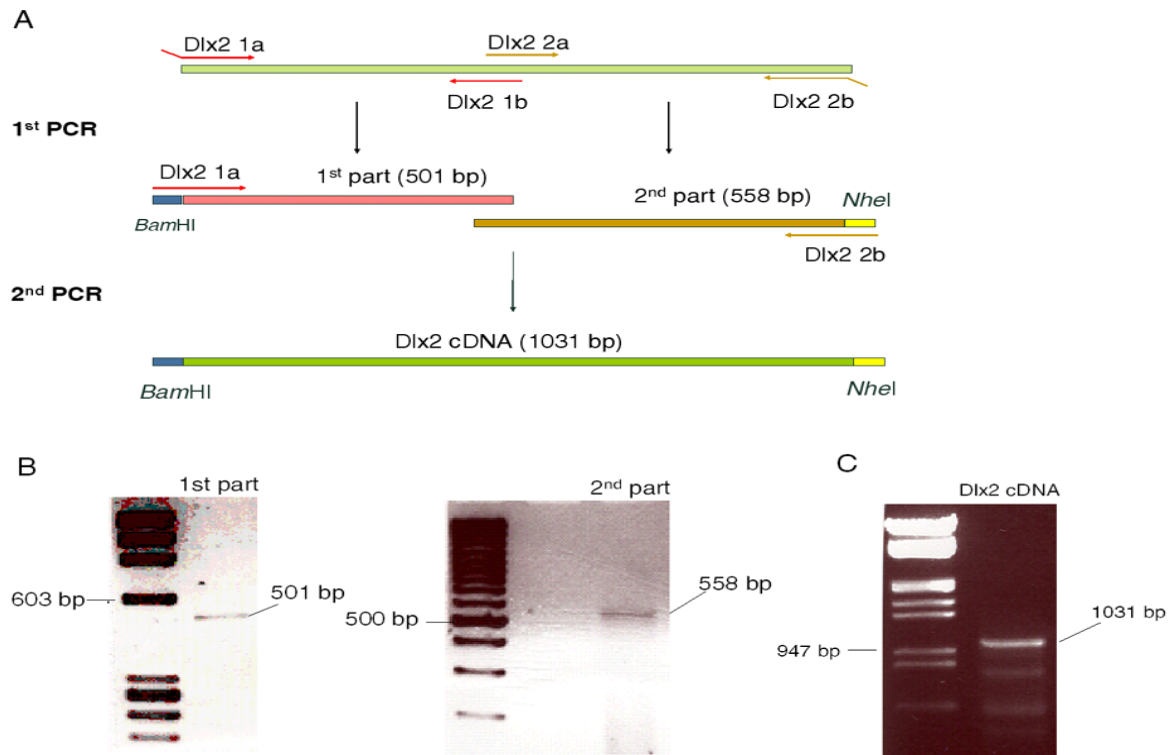


**Fig 2.1. Amplification of *Dlx2* cDNA by RT-PCR**

(A) Schematic drawing of PCR procedure showing *Dlx2* cDNA (1031 bp) is amplified by two steps of PCR using indicated primers as shown in (A). (B) Gel photos of two parts of *Dlx2* cDNA amplified by 1<sup>st</sup> PCR and (C) gel photo of complete *Dlx2* cDNA amplified by 2<sup>nd</sup> PCR are shown. Two restriction sites (*Bam*HI and *Nhe*I) were introduced at each ends of *Dlx2* gene and stop codon was deleted by primers (*Dlx2* 1a and *Dlx2* 2b).

#### 2.2.1.11.2. Cloning of *Dlx2* into lentiviral plasmid

First, the *Dlx2* cDNA was cloned to pFUGW (Lois C. 2002 Science). After *Bam*HI and *Nhe*I digestion and gel purification, the cDNA was ligated into the *Bam*HI–*Nhe*I sites of pFUGW vector so that *Dlx2* cDNA is inserted between ubiquitin-C promoter and enhanced green fluorescence protein (GFP) gene (hereafter named as plasmid for pLV *Dlx2*GFP; Fig 2.2G). pLV *Dlx2*GFP was checked by restriction analysis (Fig 2.2F) and

was sequenced by GATC Biotech AG. The *Dlx2* cDNA was cloned to another lentiviral vector, pLenti6 CITE EGFP (modified from pLenti6/V5DEST, Invitrogen; (Oh-hora M 2003) by Gateway cloning technology (Invitrogen). The *attB*-containing *Dlx2* cDNA was amplified by PCR (Fig 2.2A) and was purified by gel extraction and was cloned to donor vector (pDONR221, Invitrogen) by BP recombination reaction (Fig 2.2A, Invitrogen). After BP recombination, pDONR *Dlx2* was propagated in *E.coli* DH5 $\alpha$  by negative selection with *ccdB* gene which has lethal effect in most *E. coli* strains (Bernard P 1992) and is replaced with *Dlx2* gene by recombination. Minipreps plasmids were prepared by selecting randomly four colonies and were analysed by restriction of *NheI* site. The pDONR221 is restricted to two fragments (4496 bp and 266 bp) (Fig 2.2D, line 5) and the pDONR221*Dlx2* to two fragments (3283 bp and 266 bp) with different size (Fig 2.2D, line 1~4). As shown in Fig 2.2D, four colonies were all positive, showing high efficiency of recombination and negative selection. In a similar way, the *Dlx2* gene of pDONR221*Dlx2* was then cloned to pLenti6 CITE EGFP by LR recombination reaction (Fig 2.2B, Invitrogen) and the construct was named as pLV *Dlx2* (Fig 2.2G). pLV *Dlx2* was checked by restriction analysis (Fig 2.2E) and was sequenced by GATC Biotech AG.

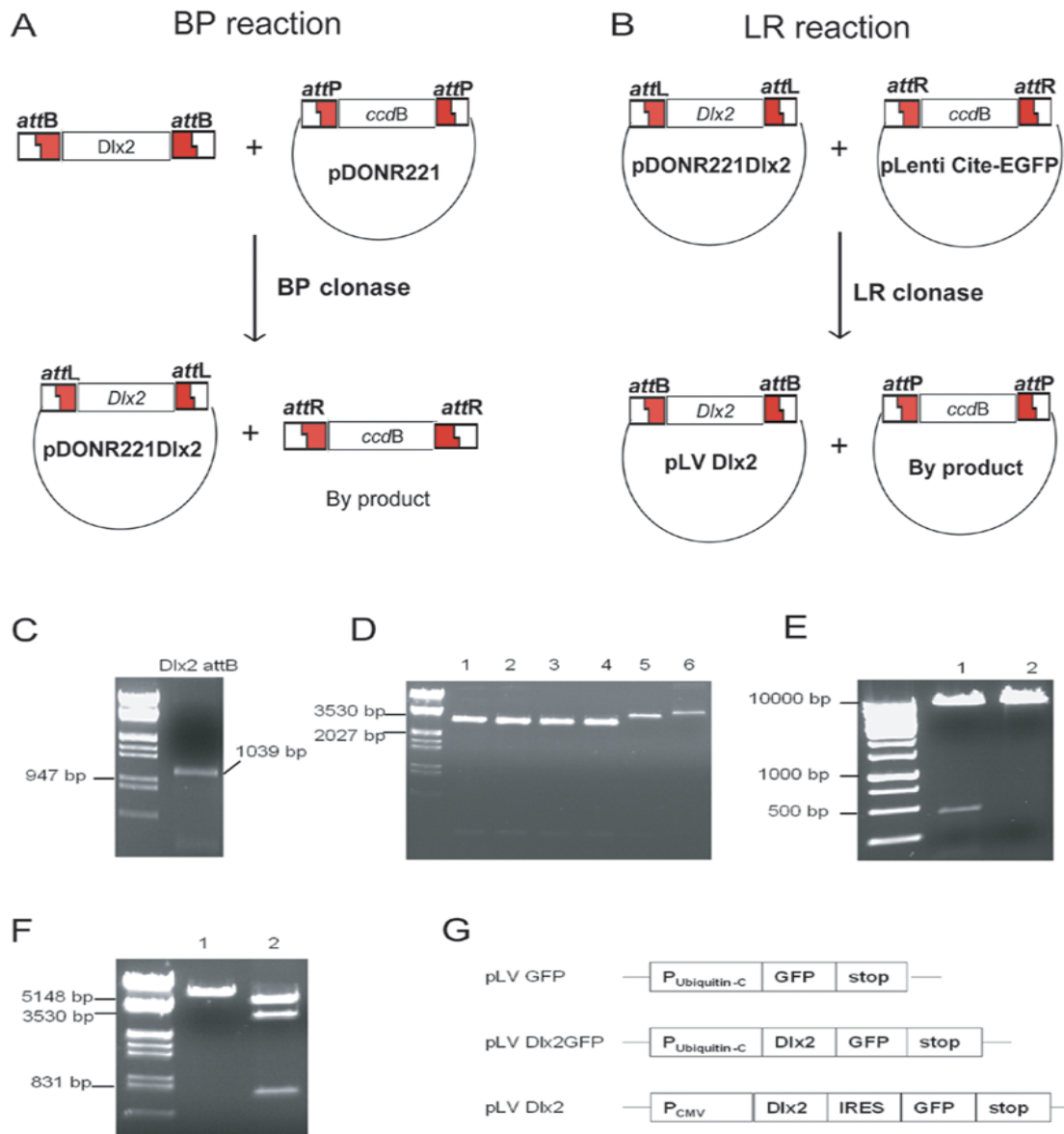


**Fig 2.2. Cloning of lentiviral constructs**

(A-E) pLV Dlx2 by Gateway cloning. (A and B) Schematic drawing showing two steps of recombination reactions of Gateway cloning. (A) PCR-amplified *attB*-containing *Dlx2* cDNA was replaced with *ccdB* gene of donor vector, pDONR221 by BP recombination reaction. (B) *Dlx2* in pDONR221 was then replaced with *ccdB* gene in pLenti Cite-EGFP by LR recombination reaction and it was named to pLV Dlx2. (C) Gel photo of PCR-amplified *attB*-containing *Dlx2* cDNA. (D) Restriction analysis of pDONR221Dlx2 by *NheI*. Lane 1-4 indicates mini-preps plasmids from randomly selected colonies after BP recombination. Lane 5 and 6 indicate pDONR221 digested by *NheI* and non-digested, respectively. (E-F) Restriction analysis of lentiviral constructs.

(continued Fig 2.2) (E) Lane 1, pLenti Cite-EGFR and Lane 2, pLV Dlx2 was restricted by *EcoRI*. (F) Lane 1, pFUGW and Lane 2, pLV Dlx2GFP was restricted by *SmaI*. All restriction analysis showed DNA bands at expected sizes. (G) Schematic drawing of lentiviral plasmids used in the experiment.

### 2.2.2. Methods in Proteins

#### 2.2.2.1. Cell lysis for protein

Cell culture was spined down and the supernatant was discarded. Cells were lysed by adding 100  $\mu$ l of preheated sample buffer and boiled at 95 °C for 5 min. It was vortexed several times during heating time. After heating, cell lysates were cooled down on ice until loading to SDS PAGE.

#### Sample buffer (2x)

Glycerol	30 ml
20% SDS	20 ml
1M Tris (pH 6.8)	16 ml
0.2% bromophenol blue	10 ml
H <sub>2</sub> O	filled up to 100 ml

\* DTT was added to a final concentration of 1 mM just before use.

**2.2.2.2. SDS PAGE**

SDS discontinuous polyacrylamide gel electrophoresis was prepared for separating all proteins in size. For this, 10% resolving gel and 5% stacking gel and running buffer were prepared as described below. The cell lysates were boiled in sample buffer for 5 min at 95 °C and were on ice until loading. The prestained protein molecular weight marker (Fermentas) was used for protein size marker. The electrophoretic separation was carried out at a constant current of 80 mA/gel (vertical slab gel, 1.5 mm x 14 cm x 14 cm). Following this, the gel was subjected to a western blotting.

<b>Resolving gel buffer (4x):</b>	1.5 M Tris-HCl pH 8.8	181.71 g/l
	0.4% SDS	4.00 g/l
<b>Stacking gel buffer (4x):</b>	0.5 M Tris-HCl pH 6.8	60.55 g/l
	0.4% SDS	4.00 g/l
<b>Running buffer (10x)</b>	190 mM glycine	142.63 g/l
	25 mM Tris	30.27 g/l
	0.1% SDS	10.00 g/l
<b>Resolving gel (10%, 20 ml)</b>	40% Acrylamide/Bis	5 ml
	Resolving buffer (4x)	5 ml
	H <sub>2</sub> O	9.8 ml
	APS (100x)	200 ul
	TEMED (1000x)	20 ul
<b>Stacking gel (5%, 8ml)</b>	40% Acrylamide/Bis	1 ml
	Resolving buffer (4x)	1 ml
	H <sub>2</sub> O	5.9 ml
	APS (100x)	80 ul
	TEMED (1000x)	8 ul

### 2.2.2.3. Western Blot

Following electrophoresis, proteins in a polyacrylamide gel were transferred to a nitrocellulose membrane by wet electroblotting. The gel and membrane are sandwiched between two stacks of filter paper that have been pre-wetted with transfer buffer. The membrane is placed near the anode, and the gel is placed near the cathode. SDS-coated, negatively charged proteins are transferred to the membrane when an electric current is applied. To control protein transfer, the nitrocellulose membrane was stained in Ponceau S for 1 min and then washed with dH<sub>2</sub>O. At this step the nitrocellulose can be dried. The protein-blotted nitrocellulose was then washed twice for 10 min each time in 15 ml PBST buffer and incubated overnight in blocking solution at 4 °C. The membrane was washed briefly in PBST buffer and incubated in primary antibody solution for 1 hour at room temperature. The membrane was washed again three times in PBST buffer for 10 min each time at room temperature and incubated in secondary antibody solution for 1 hour at room temperature. The membrane was washed in the same way and was ready for chemiluminescent detection. The chemiluminescent reagent was freshly prepared by mixing enhanced luminol reagent and oxidizing reagent with 1:1 ratio. The reagent was simply spread on the membrane and incubated around 1~3 min. After removing the excess of reagent the membrane was covered with thin plastic wrap and exposed to X-ray film with variable exposure time (1~40 min) in darkness. Finally the film was developed by using an automated film developer.

<b>Transfer buffer (10X)</b>	150 mM Glycine	112.6 g/l
	20 mM Tris	24.2 g/l
	0.1% SDS	10.0 g/l
	20% Methanol	

PBST 0.1% (v/v) Tween 20 in PBS

Blocking solution 5% non fat milk powder in 1x PBST

\* Primary and secondary antibody were prepared in 3~5% non fat milk powder PBST.

### **2.2.3. Lentiviral production and transduction**

Replication-incompetent lentivirus was produced from HEK293FT cells by lipofectamin-mediated cotransfection of three plasmids (see method 2.2.5.2.3). Briefly, HEK293FT cells cultured in growth medium (see Method 2.2.5.2.1) were cotransfected with 7.5  $\mu\text{g}$  lentiviral packaging plasmid, pCMVdelta8.9, 5  $\mu\text{g}$  pseudotyping plasmid pVSVG (Naldini L 1996; Zufferey R 1997) and 1  $\mu\text{g}$  lentiviral expression plasmid in 10 cm plates (NUNC). Viral supernatant was collected ~65 hours after transfection, centrifuged at low speed and filtered through a 0.45  $\mu\text{m}$  low-protein-binding PVDF filter (Millipore), aliquoted and stored at  $-80\text{ }^{\circ}\text{C}$ .

aSVZ or hippocampal cells were infected in a 1:1 mixture of DMEM (4.5 g/l) and F12 medium (Gibco) supplemented with 5% FCS, 0.05 mM MEM Non-essential Amino Acids, 25  $\mu\text{M}$  sodium pyruvate, 2% B27 and growth factors, 10 ng/ml FGF-2 and 20 ng/ml EGF with cell density, 250000 cells/ml,  $5.2 \times 10^4$  cells/cm<sup>2</sup> in 6-well plate (NUNC). After 4~5 hours, cells were plated with cell density, 200000 cells/ml,  $5.2 \times 10^4$  cells/cm<sup>2</sup> in Euromed-N basal medium supplemented with 100 U/ml Penicillin/Streptomycin, 2 mM L-glutamine, 2% B27 and growth factors, 10 ng/ml FGF-2 and 20 ng/ml EGF, hereafter referred as E/F medium. Four to five days later, infected cells were sorted by flow cytometry based on green fluorescence protein

expression and/or EGFR levels. In the latter case prior to sorting, EGF was not added to the growth medium.

### **2.2.4. Tissue dissection**

Brains were obtained from day 7 postnatal (P7) CD1 (Charles River) albino mice or CB57 BL/6 and prenatal mouse embryos at day 18 (E18) of embryonic development (plug day = E1). Time-mated pregnant (plug day=1) dams were killed by increasing CO<sub>2</sub> concentrations followed by neck dislocation, whereas P7 animals were killed by decapitation, in accordance with the local ethical guidelines for the care and use of laboratory animals (Karlsruhe, Germany). The aSVZ and the hippocampus were dissected from P7 mouse brains in cold sucrose solution. Dissected tissues were then incubated in papain solution at 37 °C. After 10~15 min, the papain solution was removed and enzymatic digestion was stopped by washing the tissue in Euromed-N basal medium containing 0.7 mg/ml ovomucoid and 20 U/ml DNase. Dissociated cells were plated in growth medium with or without prior infection. For micro-dissection of the hippocampus, brains were dissected in ice-cold Krebs buffer. Dissected brains were covered with 4% low-melting agarose gel in PBS at ~40 °C and then immediately placed at 4 °C to harden the agarose solution. Afterwards brains were sliced on a vibratome (HM650V, Microm, Germany) into 300 µm coronal section in ice-cold Krebs buffer. Under a dissecting microscope, hippocampal SVZ and DG regions were precisely dissected from the brain sections with fine surgical forceps.

For the embryonic tissue (E18), the GE and the hippocampus were dissociated mechanically instead of enzymatic treatment in sorting medium (see 2.2.7). On the same day, EGFR<sup>high/low</sup> cells were sorted to lysis buffer for RNA extraction (see 2.2.1.1.5).

### **Krebs buffer**

126 mM	NaCl
2.5 mM	KCl
1.2 mM	NaH <sub>2</sub> PO <sub>4</sub> ·H <sub>2</sub> O
1.2 mM	MgCl <sub>2</sub>
2.5 mM	CaCl <sub>2</sub>
11 mM	Glucose
10 mM	Hepes

### **Papain solution (in PBS)**

2.5 U/ml	Papain
0.6%	Glucose

### **Sucrose solution**

150 mM	Sucrose
125 mM	NaCl
3.5 mM	KCl
1.2 mM	NaH <sub>2</sub> PO <sub>4</sub> ·H <sub>2</sub> O
2.4 mM	CaCl <sub>2</sub> ·2H <sub>2</sub> O
1.3 mM	MgCl <sub>2</sub> ·6H <sub>2</sub> O

0.1%	Glucose
2 mM	Hepes

## 2.2.5. Cell culture

### 2.2.5.1. Bacterial cell culture

The *E. coli* was cultured at 37°C on LB agar plate or liquid LB medium with vigorous shaking at 120 rpm. Ampicillin (100 µg/ml) or kanamycin (50 µg/ml) was added for selection of transformants.

<b>Strains</b>	<i>Escherichia coli</i> DH5α <i>Escherichia coli</i> Stbl3™ (Invitrogen)
<b>LB medium</b>	10 g tryptone 5 g yeast extract 10 g NaCl in 1 L deionized H <sub>2</sub> O adjusted pH 7.0 1.5% agar was added for agar plates.

### **2.2.5.2. HEK293FT cell culture**

#### **2.2.5.2.1. Cell line and culture conditions**

The HEK293FT cell line stably expressing the SV40 large antigen from pCMVSPORT6TA<sub>g</sub>.neo plasmid, is derived from the HEK293F cell line which is a permanent line established from primary embryonic human kidney transformed with sheared human adenovirus type 5 DNA (Graham FL 1977; Harrison T 1977).

HEK293FT cells were cultured in growth medium at 37 °C in 5% CO<sub>2</sub> atmosphere with saturating humidity. Cells were trypsinized with trypsin-EDTA every 2~3 days before becoming confluent. HEK293FT cells stably express the neomycin resistance gene from pCMVSPORT6TA<sub>g</sub>.neo and maintained in growth medium containing Geneticin at the concentration, 50 µg/ml.

#### **Growth medium**

Dulbecco's MEM (4.5 g/l glucose)

10% FCS

0.1 mM MEM Non-essential Amino Acids

50 µM sodium pyruvate

50 µg/ml Geneticin

#### **2.2.5.2.2. Freezing and thawing cells**

For a storage of cells, 70~90% confluent cells were trypsinized with trypsin-EDTA for 5 min. After removing trypsin-EDTA by pipetting, the rest of cells were resuspended with 1~2 ml cold freezing medium. The cells in freezing medium were aliquoted to

cryovials with 500  $\mu$ l. The cells were then stored at  $-80\text{ }^{\circ}\text{C}$ . When cells are necessary, the frozen cells were thawed quickly at  $37\text{ }^{\circ}\text{C}$  water bath and then transferred to 10 cm plate containing growth medium. On the next day, Geneticin was added in the cell culture.

### **Freezing medium**

90% Growth medium

10% DMSO

### **2.2.5.2.3. Transfection**

One day before transfection, HEK293FT cells were trypsinized and were plated without any antibiotics into 10 cm plates to make them 70~90% confluent on the day of transfection. Before transfection, the growth medium was replaced with 5 ml fresh growth medium. Plasmid DNA (2~13.5  $\mu$ g) was diluted in 1 ml OPTI-MEM I without serum. Separately, Lipofectamine 2000 (6~40  $\mu$ l) was diluted in 1 ml OPTI-MEM I with serum. The amount ratio of DNA and lipofectamine was 1:3 (DNA:lipofectamine). After 5 min incubation at room temperature, the diluted plasmid DNA was then combined with the diluted lipofectamine 2000 and it was mixed gently and was incubated at room temperature for 20 min to allow DNA-Lipofectamine 2000 complex to form. The formed complex was added directly to cell culture. Cells were then incubated overnight at  $37\text{ }^{\circ}\text{C}$  in a 5%  $\text{CO}_2$  incubator and on the next day, the medium was replaced with growth medium without antibiotics.

### **2.2.5.3. Primary neural precursor cell (NPC) culture**

Neural precursor cells obtained from dissecting the aSVZ and the hippocampus of postnatal day 7 (P7) CD1 albino mice were cultured in growth E/F medium. After infection of cells, neural precursor cells were cultured in growth E/F medium with a cell density,  $2 \times 10^5$  cells/ml,  $5.2 \times 10^4$  cells/cm<sup>2</sup> in 6-well plate (NUNC) for 5 days before sorting. When necessary for sorting EGFR<sup>high</sup> cells, neural precursor cells were cultured in growth F medium prior to sorting.

#### **Growth E/F medium**

Euromed-N basal serum free medium

100 U/ml Penicillin/Streptomycin

2 mM L-glutamine

2% B27

10 ng/ml FGF-2

20 ng/ml EGF

#### **Growth F medium**

Euromed-N basal serum free medium

100 U/ml Penicillin/Streptomycin

2 mM L-glutamine

2% B27

10 ng/ml FGF-2

### 2.2.6. Clonal analysis

Transduced cells and/or EGFR<sup>high</sup> or EGFR<sup>low</sup> cells were sorted and were plated at a density of 1~10 cells per well in 96-well plates containing growth E/F medium (50  $\mu$ l). Cultures were kept in the incubator for a week during which a subset of plated NPCs proliferate and give rise to clones. After 7 days, the number of clones per plate was counted and the clone size was measured by counting the average number of cells per clone. To this end, more than 20 clones were collected and dissociated in a known volume of medium and the number of cells was counted. Alternatively, the diameter of each clone was measured by the grid space occupied by the clone to obtain cross-sectional area. Around 15 clones were analyzed for one experiment. For the secondary clone formation, the clones were dissociated in sorting medium and plated again at a density of 10 cells per well to 96-well plate by FACS automated cell deposition. After 7 days, the number of clones per plate was scored. For differentiation, the clones were dissociated in growth E/F medium containing DNase and dissociated-cells were then plated onto chamber slide coated with matrigel and were incubated in growth E/F medium for 2~3 days and the medium was replaced with differentiative medium. After 5~7 days incubation, differentiated cells were fixed and were immunostained to analyze their phenotypes.

#### **Differentiative medium**

Euromed-N basal serum free medium

100 U/ml Penicillin/Streptomycin

2 mM L-glutamine

2% B27

1% FCS

10 ng/ml FGF-2

### **2.2.7. Fluorescence Activated Cell Sorting (FACS)**

Dissociated-cells from clones or dissected-tissues were resuspended in ice-cold sorting medium. For sorting of EGFR<sup>high</sup> cells, the dissociated-cells were stained by adding an equal volume of sorting medium containing (40 ng/ml) EGF-conjugated Alexa 488 or 647 as described before (Ciccolini F 2005). The cell suspension was then filtered by using polypropylene round-bottom tube with cell strainer cap (BD). Sorting gates were set by using unstained cells and cells that had been were incubated in culture medium with unlabelled EGF for at least 20 minutes previous to the staining with EGF-conjugated Alexa 488 or 647. Transduced-cells were sorted based on their GFP expression. Thus, transduced-cells were simply resuspended in ice-cold sorting medium and were filtered by polypropylene round-bottom tube with cell strainer cap (BD). Sorting gates were set by using non-transduced cells. Viable cells were revealed by propidium iodide exclusion (PI). Sorting was performed on FACS Aria (Becton Dickinson). Cells were plated with clonal cell density (1~10 cells/well) to 96-well plates containing 50 µl growth E/F medium by FACS automated cell deposition units.

### **Sorting medium**

Euromed-N basal medium/Leibovitz medium (1:1)

100 U/ml Penicillin/Streptomycin

2 mM L-glutamine

2% B27

1% FCS

10 ng/ml FGF-2

20 U/ml DNase

1 µg/ml Propidium Iodide

### **2.2.8. Immunocytochemistry**

Cells were fixed in 3% paraformaldehyde in PBS containing 4% sucrose for 15 min, rinsed twice in PBS containing 10 mM glycine and permeabilized in NP-40 (0.5% in PBS) for 5 min and rinsed twice with PBS. All was done at room temperature. After fixation, cells were incubated with primary antibodies overnight at 4 °C. Next day, cells were washed several times with PBS to washout extra primary antibody and then incubated with fluorescently labelled secondary antibodies for 1 hour. Cells were washed twice with PBS and rinsed with water to remove PBS. Excess water was removed by gently tilting and tapping the chamber-slide or coverslip on a tissue paper. 5 µl of moviol was placed on each well of a chamber-slide and a glass coverslip was gently placed on top of it. Chamber- slides or coverslips were stored at 4 °C in

darkness to preserve fluorescence. Immunostaining was analyzed using a Zeiss-Axiophot inverted microscope.

### 3. Results

#### 3.1. Comparative analysis of EGFR<sup>high</sup> cells isolated from the two main neurogenic regions

##### 3.1.1. Isolation and clonal analysis of EGFR<sup>high</sup> cells

NPCs of the aSVZ form clones in response to epidermal growth factor (EGF) and display *in vitro* self-renewal and multipotency. EGF-responsive clone-forming cells can also be isolated from the hippocampus, the second main neurogenic region in the postnatal mammalian brain; however it is not clear whether there is a relationship between these two populations of NPCs and whether their proliferation and differentiation are regulated by common mechanisms.

To further investigate this issue I first performed a comparative analysis of the characteristics of cells expressing high levels of EGF receptor (EGFR<sup>high</sup>) isolated from the two main neurogenic regions of the postnatal brain. For this, the aSVZ and the hippocampus were dissected and EGFR<sup>high</sup> cells or cells expressing low levels of EGFR (EGFR<sup>low</sup>) were isolated using fluorescence activated cell sorting (FACS) as shown at Fig 3.1A (Ciccolini F 2005). Since dissociation of the postnatal tissue requires enzymatic digestion, EGFR expression was analysed after dissociated-cells had been cultured overnight to recover cell surface expression of EGFR (Fig 3.1A). After sorting, the proliferation of NPCs within the two populations of EGFR<sup>high</sup> cells was analyzed by clonal analysis. After 7 days, the number of clones was counted and the proliferation rate of the original clone-forming cell was measured by quantifying the number of cells

in each clone (Fig 3.1B and C). The FACS analysis revealed that in both regions EGFR<sup>high</sup> cells represented only a subset of the total cell population (aSVZ: 5~8%; hippocampus: 0.5~0.8%). Although both EGFR<sup>high</sup> populations, either isolated from the aSVZ or the hippocampus, were enriched in clone forming cells (Fig 3.1B), aSVZ EGFR<sup>high</sup> cells had higher clone forming capacity and formed bigger size clones, than hippocampal EGFR<sup>high</sup> cells (Fig 3.1B and C). To compare their self-renewal capacity, primary clones were dissociated and plated for the formation of secondary clones. This analysis revealed no differences between the two groups in the incidence of cells capable of forming secondary clones (Fig 3.1D left). However, when I normalized the percentage of secondary clones (Fig 3.1D left) to the clone size (Fig 3.1D right), to calculate the total number of secondary clones generated by primary clone forming cell, I found that aSVZ EGFR<sup>high</sup> cells in a given time give rise to more secondary clone forming cells than hippocampal EGFR<sup>high</sup> cells.

Taken together, these data show that EGFR<sup>high</sup> cells isolated from the aSVZ and the hippocampus are both enriched in clone-forming NPCs. However, hippocampal EGFR<sup>high</sup> cells have a slower proliferation rate than EGFR<sup>high</sup> cells isolated from aSVZ NPCs and therefore *in vitro* the first give rise to less secondary clone forming cells than the latter.

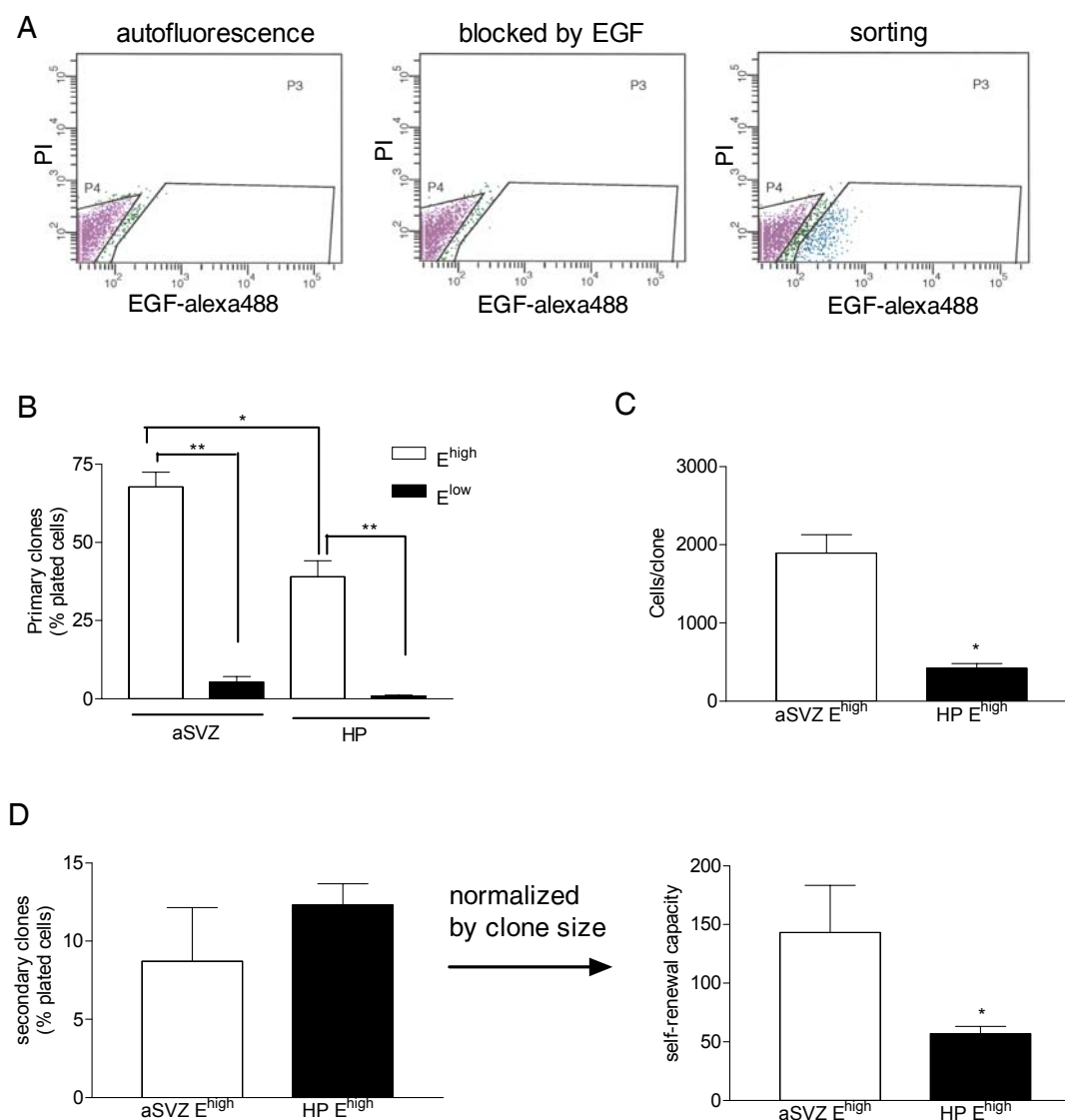


### Fig 3.1. Clonal analysis of EGFR<sup>high</sup> cells derived from the aSVZ and the hippocampus

(A) Representative FACS plots for the analysis of EGFR (E) expression as revealed by binding of EGF-alexa488. After tissue dissection and dissociation, aSVZ cells have been cultured for 24 hours and then stained with EGF-alexa488 with (central panel) or without (left panel) previous incubation with unlabelled EGF. Dead cells were excluded by propidium iodide (PI) exclusion. EGFR<sup>high</sup> ( $E^{\text{high}}$ ) and EGFR<sup>low</sup> ( $E^{\text{low}}$ ) cells are shown in P3 and P4 gates, respectively. (B) Quantitative analysis of the percentage of clone forming cells in the sorted populations based on the levels of EGFR expression. Though selection of EGFR<sup>high</sup> cells allows to enrich clone-forming NPCs independently of the brain region, aSVZ EGFR<sup>high</sup> cells are more clonogenic than hippocampal

(continued Fig 3.1) EGFR<sup>high</sup> cells. (C) Quantitative analysis of the number of cells per clone shows that hippocampal EGFR<sup>high</sup> cells proliferate slower than aSVZ EGFR<sup>high</sup> cells. (D) Quantitative analysis of the secondary clone formation. Primary clones were dissociated to single cells and were plated again at clonal density by FACS cell deposition to allow the formation of secondary clones. The relative and total number of secondary clones generated are shown in the right and left panel, respectively. Data represent the means  $\pm$  SEM of at least three independent experiments (\*\*,  $P < 0.01$ ; \*,  $P < 0.05$ ).

### 3.1.2. Localization of clone-forming cells within the hippocampus

It is well established that neurogenesis occurs in the dentate gyrus (DG) subgranular zone (SGZ) of the hippocampus throughout life (Alvarez-Buylla et al., 2002; Gage 2000). However, previous studies have shown that the majority of clone-forming cells within the hippocampus reside in the hippocampal SVZ (hSVZ) but not in the DG (Seaberg RM 2002). To further characterize hippocampal NPCs, I investigated the subregional localization of clonogenic NPCs within the postnatal hippocampus. To this end, I microdissected the dentate gyrus and the hSVZ adjacent to the CA1 region, from vibratome coronal telencephalic sections and analysed the clone forming ability of the cells derived from these two subregions (Fig 3.2A). Clonal analysis revealed a 10-fold higher frequency of clone forming cells in hSVZ dissociated cells than in the DG (Fig 3.2B). Since my previous data show that EGFR<sup>high</sup> cells are particularly enriched in clone-forming NPCs, I next analyzed whether the hSVZ contains more EGFR<sup>high</sup> cells than the DG. FACS analysis showed that, even after overnight culturing in medium containing FGF-2 which is known to promote EGFR expression in NPCs (Ciccolini F 1998), cell suspensions derived from the DG contained very few EGFR<sup>high</sup> cells

( $0.9 \pm 0.5\%$ , Fig 3.2C and D). In contrast, in cultures from the hSVZ, EGFR<sup>high</sup> cells represented  $7.8 \pm 2.1\%$  of the total cell population (Fig 3.2C and D). Taken together, these data show that within the hippocampus most EGFR<sup>high</sup> cells and clone-forming cells are localized in the hSVZ.

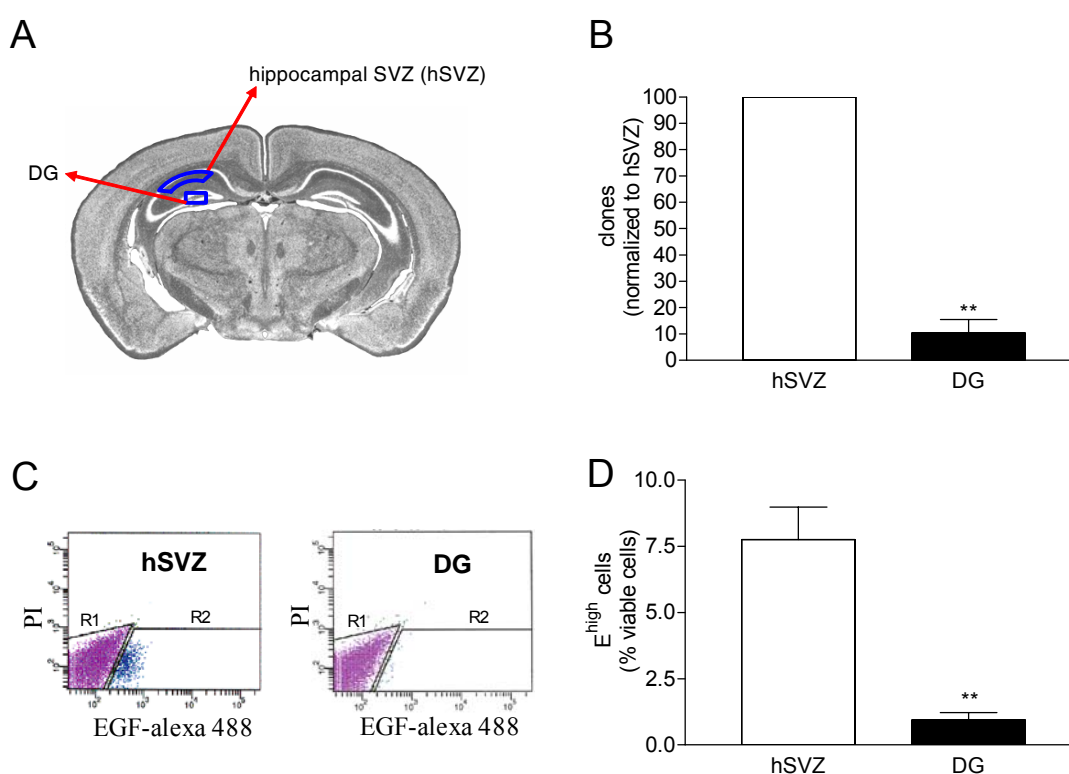


**Fig 3.2. Clonogenic cells in the hippocampus at postnatal day 7 are mostly localized in the hippocampal subventricular zone (hSVZ)**

The dissected subregions, hSVZ and DG of the hippocampus, are shown in (A). (B) Quantitative analysis of the percentage of clone-forming cells in plated hSVZ and DG cells. (C) Representative FACS plots measuring cell surface expression of EGFR in hSVZ and DG cells that after dissection and enzymatic dissociation had been cultured overnight in FGF-2 containing medium. EGFR is measured by binding of EGF-alexa488. EGFR<sup>low</sup> and EGFR<sup>high</sup> are shown in R1 and R2, respectively. Quantification of EGFR<sup>high</sup> cells is shown in (D). Numbers represent the means  $\pm$  SEM of at least three independent experiments (\*\*,  $P < 0.01$ ).

### 3.1.3. Origin of hippocampal EGFR<sup>high</sup> cells

From early (E11) to late embryonic development (E18) subsets of cells generated within the ganglionic eminences (GE) migrate dorsally along tangential routes of cell migration to the cortex and the hippocampus where they give rise to GABAergic interneurons (Anderson SA 2001). Since most GABAergic interneurons in the hippocampus derive from precursors of the medial ganglionic eminence (MGE) characterised by the expression of *Nkx2.1* (Pleasure SJ 2000), I investigated the possibility by semiquantitative reverse transcription (RT) PCR that hippocampal EGFR<sup>high</sup> cells express *Nkx2.1*. As shown in Fig 3.3, *Nkx2.1* specific transcript was detected not only in EGFR<sup>high</sup> and EGFR<sup>low</sup> cells isolated from the GE, but also in EGFR<sup>high</sup> cells derived from the hippocampus, whereas *Nkx2.1* transcript was rarely detected from RNA extracted from hippocampal EGFR<sup>low</sup> cells. This data suggests that at least a subset of EGFR<sup>high</sup> cells may migrate from the basal GE to the hippocampus during embryonic development.



#### Fig 3.3. Expression of *Nkx2.1* in hippocampal EGFR<sup>high</sup> cells

*Nkx2.1* expression is analyzed by semiquantitative RT-PCR in dissociated cells of the E18 ganglionic eminence (GE) and hippocampus (HP) that had been sorted by FACS on the basis of EGFR (E) expression. The endogenous *Gapdh* gene was used for normalization. Note that *Nkx2.1* expression is detected not only in GE EGFR<sup>high/low</sup> cells but also in hippocampal EGFR<sup>high</sup> cells.

### 3.1.4. Differential expression of genes associated with transit-amplifying cells between EGFR<sup>high</sup> cells isolated from the GE and the hippocampus

Most EGFR<sup>high</sup> cells in the postnatal aSVZ represent transit-amplifying cells (TAPs, Type C), one of three main precursor types (Type B, C and A), driving the process of adult neurogenesis in this region. However it is not known whether EGFR<sup>high</sup> cells in the hippocampus have similar functional properties. I here found that hippocampal EGFR<sup>high</sup> cells share many characteristics with EGFR<sup>high</sup> cells derived from the aSVZ. For example, they are both located in the SVZ, express MGE marker such as *Nkx2.1* and can form clones mainly in response to EGF. I therefore next investigated whether they also express DLX2 and EGFR, whose co-expression identifies type C cells in the aSVZ, at the same level of aSVZ EGFR<sup>high</sup> cells. Thus, I used quantitative reverse transcription (qRT) PCR to quantify levels of *Egfr* and *Dlx2* mRNAs in the cell populations. Consistent with the pattern of EGFR protein expression revealed by FACS analysis (Fig 3.4A-D), *Egfr* mRNA was found in both hippocampal and GE EGFR<sup>high</sup> cells, albeit at different levels. Compared to EGFR<sup>high</sup> cells derived from the GE, expression of *Egfr* mRNA was significantly lower in hippocampal EGFR<sup>high</sup> cells (Fig 3.4E). Interestingly, even greater difference was observed between the two cellular subsets in the expression of *Dlx2* (Fig 3.4E). Indeed this analysis revealed that respect to GE EGFR<sup>high</sup> cells, expression of *Dlx2* is drastically lower in hippocampal EGFR<sup>high</sup> cells. Thus, despite they are both localized to the SVZ and both originate from basal GE, hippocampal and GE EGFR<sup>high</sup> cells differ not only in proliferation rate but also display a different pattern of gene expression.

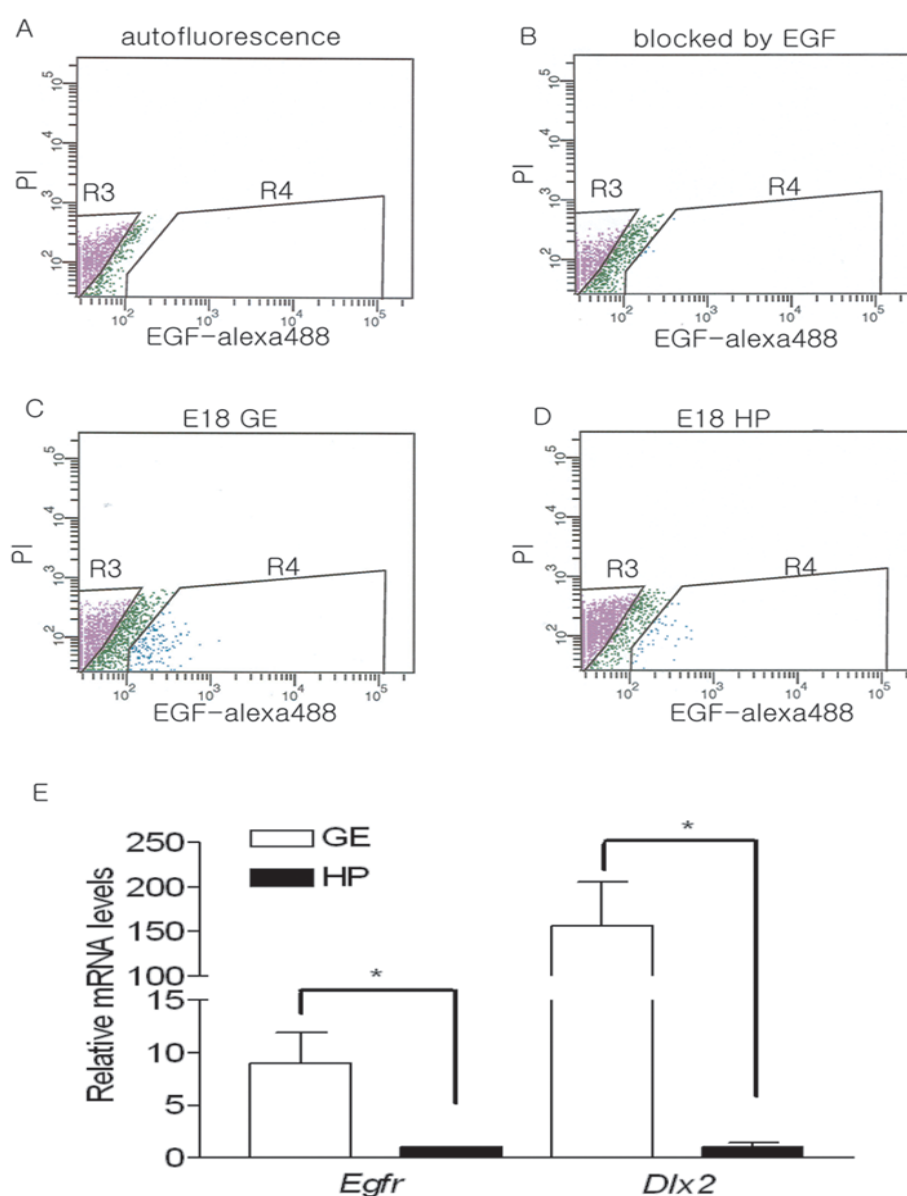


**Fig 3.4. Quantitative analysis of *Egfr* and *Dlx2* mRNA levels in E18 EGFR<sup>high</sup> cells sorted by FACS**

(A-D) Representative FACS plots for sorting EGFR<sup>high</sup> cells derived from the GE and the hippocampus of E18. After tissue dissection and dissociation, cells were then stained with EGF-alexa488 with (B) or without (C, D) previous incubation with unlabelled EGF. The plot (A) indicates cells without staining of EGF-alexa488. Dead cells were excluded by propidium iodide (PI) exclusion. EGFR<sup>high</sup> and EGFR<sup>low</sup> cells are shown in R3 and R4 gates, respectively. (E) Quantification of mRNA by qRT-PCR. Total RNA was extracted from EGFR<sup>high</sup> cells sorted by FACS and relative gene expression levels of *Egfr* and *Dlx2* were quantified by qRT PCR. Numbers represent the ratio between GE

(continued Fig 3.4) and HP mRNA levels, which are both normalized to the respective mRNA levels of endogenous gene *beta-2 microglobulin* ( $\beta 2M$ ). Note that both *Egfr* and *Dlx2* mRNA levels are higher in GE EGFR<sup>high</sup> cells than hippocampal EGFR<sup>high</sup> cells. Numbers represent the means  $\pm$  SEM of at least three independent experiments (\*,  $P < 0.05$ ).

### 3.2. Lentivirus-mediated *Dlx2* gene delivery and expression

The above data showed that despite being both clonogenic and localized in the germinal epithelium lining the lateral ventricle, hippocampal EGFR<sup>high</sup> cells are less clonogenic and self-renewing, and express lower level of *Dlx2* than their counterpart isolated from the GE. Since DLX2 is expressed in Type C cells of postnatal aSVZ that are also capable of undergoing clone formation, I next attempted to manipulate DLX2 expression in NPCs derived from these two different neurogenic regions in postnatal mouse brain, the aSVZ and the hippocampus, using a lentivirus-mediated gene delivery system. For this, I cloned cDNA encoding the murine DLX2 protein, (Accession number, NM\_010054) into the pFUGW (Lois C. 2002 Science) and pLenti6 CITE EGFP (Oh-hora M 2003) lentiviral backbones to obtain expression of DLX2 and GFP as a fusion protein or two proteins, respectively (see materials and methods 2.2.1.11).

To investigate the effectiveness of this approach to modulate DLX2 expression, I transduced HEK293FT cells with LV GFP, LV Dlx2GFP or LV Dlx2. Four days after infection, transduced-HEK293FT cells were sorted on the basis of GFP expression by FACS and then processed for protein and RNA extraction to analyse the expression levels of GFP and DLX2 (Fig 3.5). In western blot, both GFP and DLX2 antibodies revealed a band of ~72 kDa in LV Dlx2GFP-infected HEK293FT cells showing their

expression as a fusion protein, whereas in LV GFP-infected HEK293FT cells GFP antibodies revealed a single band of ~29 kDa corresponding to the size of GFP protein (Fig 3.5A). To analyse levels of DLX2 and GFP expression in single NPCs, I used DLX2 antibodies to immunostain aSVZ NPCs that had been previously transduced with LV GFP or LV Dlx2GFP. As shown in Fig 3.5B fluorescence levels of DLX2 were much higher in LV Dlx2GFP-transduced than in LV GFP-transduced NPCs which only expressed endogenous levels of DLX2. The same analysis was attempted with LV Dlx2. However, due to very low infection rate of LV Dlx2 (LV GFP, 50~90%; LV Dlx2GFP, 2~10%; LV Dlx2, 0.5~2%), it was difficult technically to sort enough number of cells transduced with LV Dlx2. For this reason, I next analyzed mRNA levels of *Dlx2* between the control and *Dlx2*-transduced HEK293FT cells. Total RNA was extracted from HEK293FT cells infected by each lentivirus. RT-PCR was done with the same amount of RNA and normalized by endogenous gene expression of *Gapdh*. As shown in Fig 3.5C, when the PCR reaction was performed under stringent conditions (i.e. high annealing temperature, 63 °C), the GFP transcript was amplified in HEK293FT cells transduced with either lentiviral construct, whereas the *Dlx2* transcript was amplified only from HEK293FT cells transduced with LV Dlx2GFP or LV Dlx2. However, using the same Dlx2 primers in less stringent conditions (i.e. low annealing temperature, 56 °C), a band was also observed in HEK293FT cells that had been transduced with LV GFP (not shown). However, the amplified band was slightly smaller than the *Dlx2*-specific band. Since human *DLX2* can be amplified in a case that HEK293FT cells express *DLX2*, I compared the sequence of Dlx2 gene between murine and human to check whether primers used in this experiment also matches with human *DLX2*. It showed that although forward primer matches 100% with both human and murine Dlx2,

the reverse primer does not match well with human *DLX2* but partly. Moreover, the comparison revealed that human *DLX2* transcript would be amplified by RT-PCR with the size of 139 bp, which is 20 bp smaller than mouse *Dlx2* specific band, 159 bp. Thus, the smaller band in the control GFP-transduced cells would be from amplification of the endogenous human *DLX2* mRNA.

By qRT-PCR, the mRNA level of *Dlx2* was also analyzed from clones formed by transduced-NPCs. To this end, total RNA was extracted from primary clones formed by aSVZ precursors transduced by lentiviral construct. Consistently, this analysis revealed that aSVZ precursors transduced by either DLX2-expressing lentiviral construct expressed more *Dlx2* transcript, compared to the control GFP-transduced NPCs (Fig 3.5D; Dlx2GFP,  $39 \pm 14$  times; Dlx2,  $14 \pm 6.7$  times higher than GFP). Taken together, these data indicate that the lentivirus constructs can be used to drive the expression of the two DLX2 recombinant proteins in NPCs.

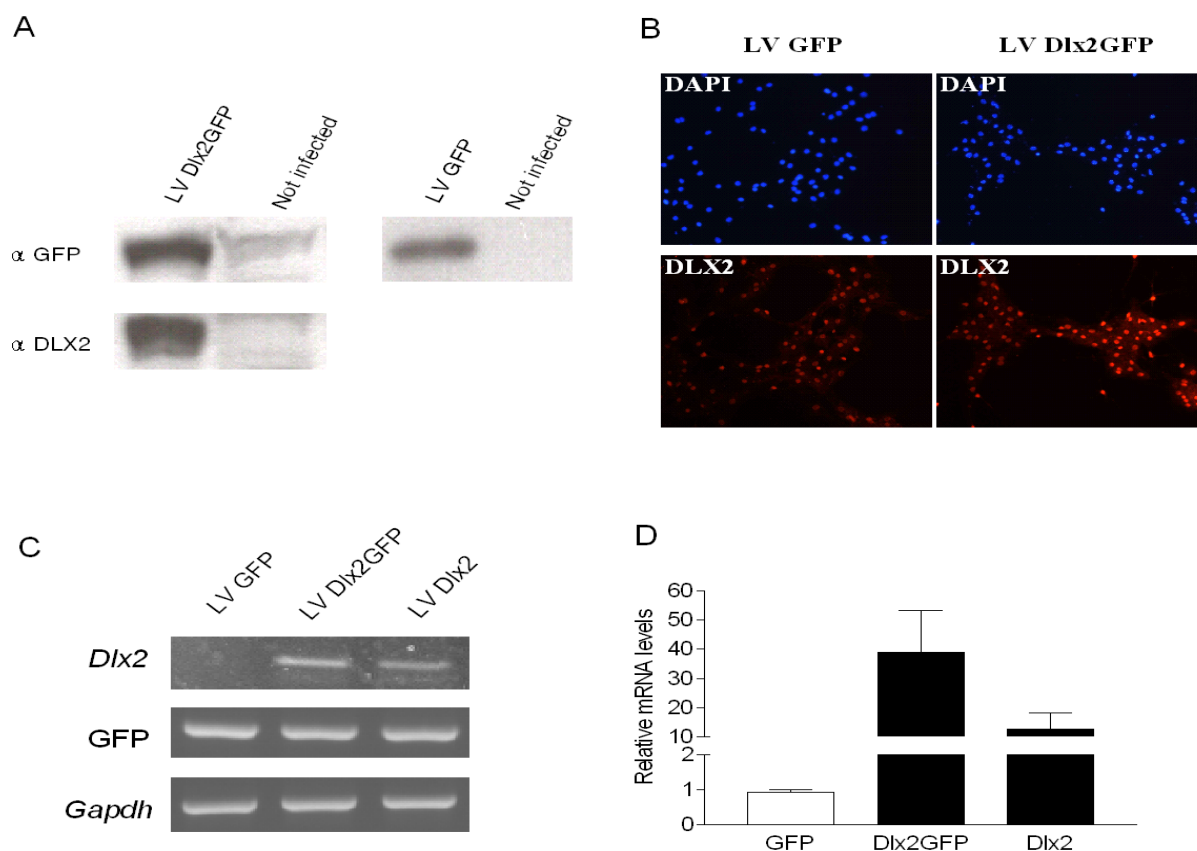


### Fig 3.5. Analysis of lentiviral-mediated gene delivery and expression

(A) Western blot analysis of DLX2 and GFP protein expression in non-transduced and transduced-HEK293FT cells with the indicated lentiviruses. (B) Detection of DLX2 protein (red) by immunocytochemistry in NPCs five days after transduction with either LV Dlx2GFP or LV GFP. Note that aSVZ precursors transduced with LV Dlx2GFP express higher levels of DLX2, compared to the endogenous levels shown in aSVZ cells transduced with LV GFP. DAPI counterstain of the nuclei is shown in blue. (C) Transgene GFP and mouse *Dlx2* mRNA expression in HEK293FT cells transduced with the indicated lentiviruses. The endogenous *Gapdh* gene was used for normalization. (D) Quantitative analysis of *Dlx2* mRNA level by qRT-PCR. Total RNA was extracted from primary clones formed by aSVZ NPCs transduced by indicated lentiviral construct and relative gene expression levels of *Dlx2* was quantified by qRT-PCR. The mRNA level of *Dlx2* was normalized by *beta-2 microglobulin* ( $\beta 2M$ ). Numbers represent the relative levels of *Dlx2* mRNA, compared to the levels of GFP-transduced cells. Note that *Dlx2*-transduced NPCs express higher levels of *Dlx2*, compared to the control GFP-transduced NPCs.

### **3.3. Effect of DLX2 over-expression on hippocampal and aSVZ NPCs**

#### **3.3.1. DLX2 increases cell proliferation rate**

To investigate the functional role of DLX2 in NPCs, I transduced dissociated postnatal aSVZ and hippocampal cells with LV Dlx2GFP, LV Dlx2 and LV GFP as control. Since cells transduced by either lentiviral construct express GFP, five days after infection and growth in culture medium containing both EGF and FGF-2 with a cell density of  $2 \times 10^5$  cells/ml, GFP-expressing cells were sorted into 96-well plates by FACS automated cell deposition (Fig 3.6A) and left them to proliferate for seven days. To determine the effect of DLX2 over-expression on cell proliferation, I analysed in each group of transduced-NPCs both the number of clones (see below 3.3.3) and the size of clone as a read out of cell proliferation. To analyze clone size, the cross-sectional area of each clone was calculated by measuring the diameter of the clone under the microscope with the aid of a graded objective. This analysis revealed that both aSVZ and hippocampal cells transduced with either DLX2 expressing lentiviral construct form bigger size of clones, compared to the control counterpart (Fig 3.6, aSVZ: Dlx2GFP, 1.6 times; Dlx2, 1.3 times bigger than GFP, hippocampus: Dlx2GFP, 2.0 times; Dlx2, 2.2 times bigger than GFP). To establish the relationship between clone size and cell number, I also analyzed the average number of cells in a clone by collecting more than 30 clones, dissociating and counting the number of cells. This analysis revealed that clones derived from Dlx2GFP-transduced aSVZ cells contain around four times more cells than clones derived from GFP-transduced cells. Thus, although the measure of cross-sectional area underestimates the number of cells in a clone, it reflects the size of

clone. Taken together, these observations suggest that DLX2 affects on clone growth by modifying the proliferation rate of clone forming cells derived from both the aSVZ and the hippocampus.

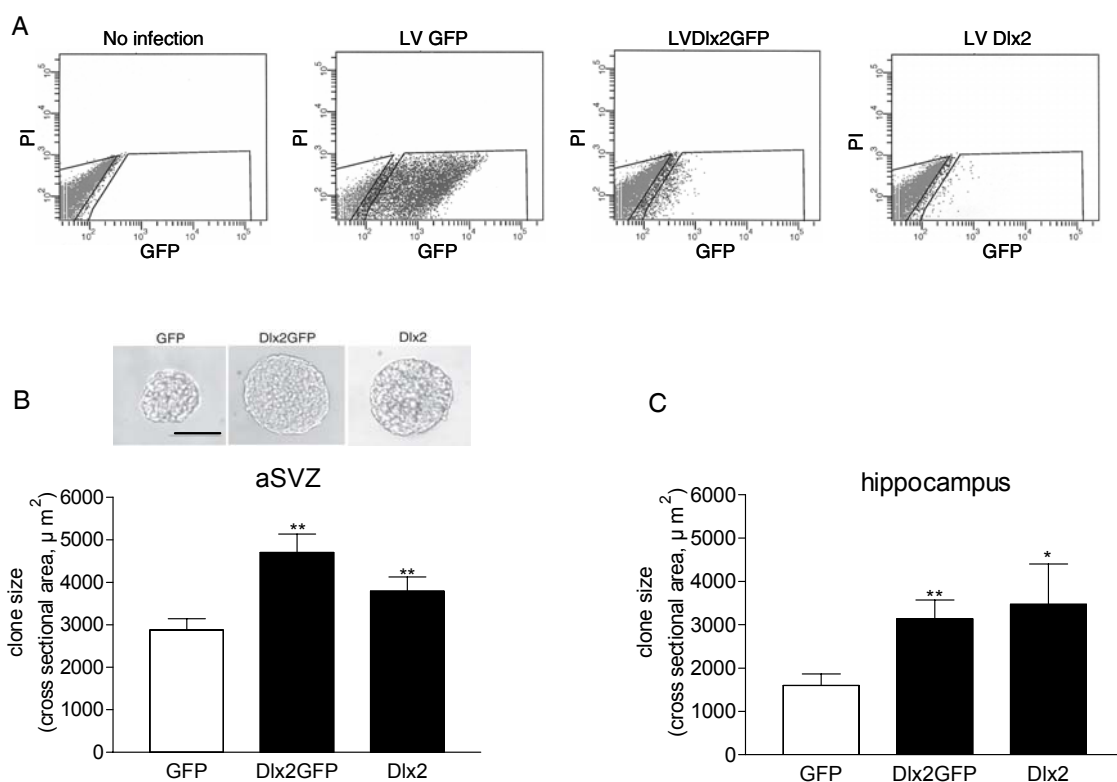


### Fig 3.6. Effect of DLX2 on clone size

(A) Representative FACS plots for isolating transduced-cells on the basis of GFP expression. GFP-expressing cells were distinguished by setting gate with non-transduced cells. Dead cells were excluded by propidium iodide staining. (B-C) Representative clone photos (scale bar is  $100\ \mu\text{m}$ ) and measurement of clone size seven days after sorting and plating of transduced-cells. More than 15 clones were analyzed for one experiment. Numbers represent the means  $\pm$  SEM of at least three independent experiments (\*\*,  $P < 0.01$ ; \*,  $P < 0.05$ ).

### **3.3.2. Effect of DLX2 over-expression on the differentiation of hippocampal and aSVZ NPCs**

I next investigated whether DLX2 over-expression affects on the differentiation of NPCs. To this end, clones derived from transduced-cells were dissociated and plated for differentiation. After 5-7 days neurogenesis in the different culture groups was analyzed by immunocytochemistry with TUJ1 antibodies, which is a marker for immature neurons (Menezes JR 1994). This analysis revealed that *Dlx2*-transduced cultures derived both from the aSVZ and the hippocampus generated more neurons than control GFP-transduced cultures (Fig 3.7). Furthermore, consistent with a previous report suggesting that DLX2 is exclusively expressed in the nucleus (Eisenstat DD 1999), in *Dlx2*GFP-transduced precursors GFP was detected only in the nucleus, whereas GFP-transduced precursors displayed GFP immunofluorescence in the whole cytoplasm (Fig 3.7).

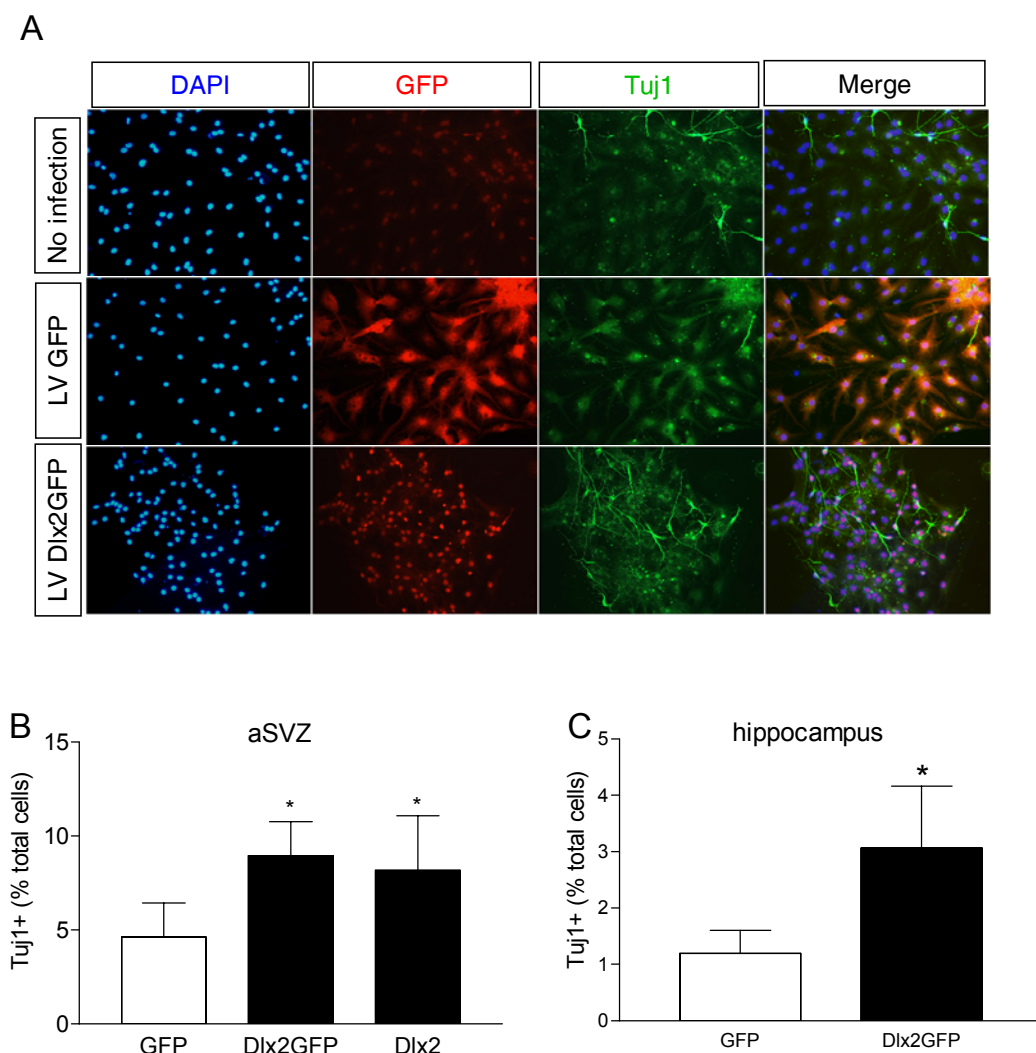


### Fig 3.7. DLX2 promotes neuronal differentiation

Dissociated clones were analyzed 5~7 days after induction of differentiation by immunocytochemistry with TUJ1 specific antibodies. (A) Representative microphotographs showing immunoreactivity to GFP (red) and TUJ1 (green) antibodies and DAPI counterstain (blue) of the nuclei in cultures of dissociated primary clones obtained from aSVZ precursors that had been transduced as indicated. (B-C) Quantitative analysis of the percentage of TUJ1+ neurons in the total cell population of Dlx2GFP and Dlx2-transduced cultures. Numbers represent the means  $\pm$  SEM of at least three independent experiments (\*,  $P < 0.05$ ).

DLX2 could promote neuronal differentiation by either increasing the number of neurogenic TAPs that upon differentiation will give rise to neuroblasts or by promoting the proliferation of neuroblasts. To investigate the mechanisms underlying the effect of DLX2 on neurogenesis, I analyzed which cell type, neuroblasts or TAPs is over represented in clones formed by DLX2-transduced precursors. To this end, I took advantage of the fact that stem cells/TAPs form more secondary clones, compared to neuroblasts. I therefore compared the ability to form secondary clones across the various groups of transduced-NPCs. This analysis revealed that clones originating from NPCs transduced with either DLX2 expressing lentivirus contained a smaller proportion of cells capable of generating clones than the control counterpart (Fig 3.8). Taken together, these data suggests that DLX2 over-expression promotes neuronal differentiation by the generation of more committed neuroblasts.

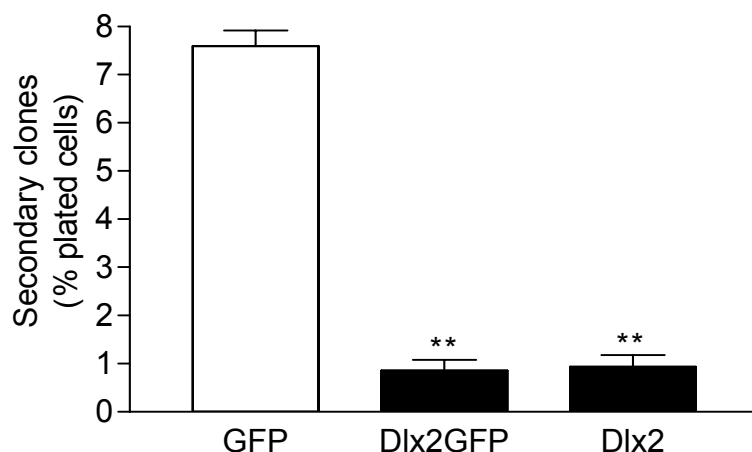


**Fig 3.8. Quantitative analysis of the percentage of plated cells undergoing secondary clone formation**

Primary clones were dissociated and plated with clonal density by FACS automated cell deposition. Numbers represent the means  $\pm$  SEM of at least two independent experiments (\*\*,  $P < 0.01$ ).

### **3.3.3. Effect of DLX2 over-expression on clone formation**

To investigate whether DLX2 expression affects the ability of NPCs to form clones, postnatal aSVZ and hippocampal cells were transduced with the lentiviral constructs (LV GFP, LV Dlx2GFP and LV Dlx2) and allowed to form clones as previously described. The number of clones formed by transduced-cells was scored after 7 days. This analysis showed that cells derived from the aSVZ upon transduction with either DLX2-expressing lentiviral constructs formed significantly more clones than control GFP-transduced cells (Fig 3.9A, GFP,  $10.3 \pm 1.29\%$ ; Dlx2GFP,  $15.4 \pm 1.8\%$ ; Dlx2,  $18.2 \pm 2.3\%$ , mean  $\pm$  SEM). In contrast, forced expression of DLX2 in hippocampal cells had no effect on clone formation (Fig 3.9B). Taken together, these data show that DLX2 over-expression has similar effects on clone size and neurogenesis of both aSVZ and hippocampal NPCs, however it leads to an expansion of the pool of clone-forming cells only when overexpressed in NPCs derived from the aSVZ, suggesting DLX2 has another distinct mechanisms on aSVZ NPCs.

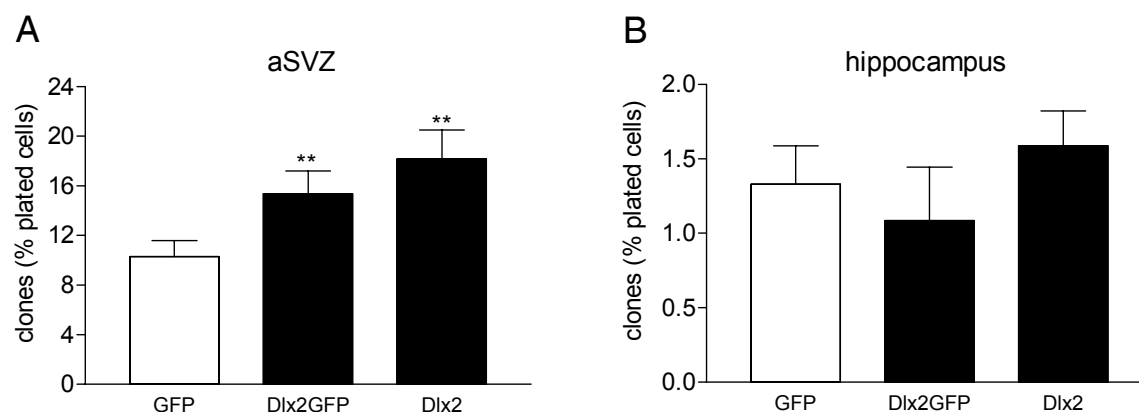


**Fig 3.9. Effect of DLX2 over-expression on the percentage of clone-forming cells present in cultures of aSVZ and hippocampal NPCs**

The number of clones formed by precursors transduced with the indicated lentiviruses was counted seven days after FACS sorting of transduced-cells to 96-well plates. Note that DLX2 over-expression increased the number of clone forming cells in cultures of aSVZ cells (A), but not in cultures of hippocampal cells (B). Numbers represent the means  $\pm$  SEM of at least three independent experiments (\*\*,  $P < 0.01$ ).

### **3.4. Mechanisms underlying the effect of DLX2 over-expression on clone formation**

#### **3.4.1. The effect of DLX2 on proliferation depends on EGFR signaling**

Next, I investigated the mechanisms underlying the increase in the number of clone-forming cells observed upon over-expression of DLX2 in aSVZ NPCs. Since EGF provides main mitogenic signals for NPCs, I tested whether the effect of DLX2 on proliferation also requires EGF. To this end, dissociated aSVZ cells were transduced with the lentiviral constructs as previously described. After five days of growth in medium containing both EGF and FGF-2, transduced-cells were sorted by FACS and were grown in medium containing both EGF and FGF-2 (E/F medium) or medium containing only FGF-2 without EGF (F medium). This analysis revealed that both the number and the size of clones generated in F medium were greatly reduced (~10 times less in the number; ~2.5 times smaller in clone size), compared to the clones obtained upon culturing in E/F medium (Fig 3.10; also see Fig 3.6B). Moreover, the effect of DLX2 on clone number and size was not observed when transduced-cells were grown only in the presence of FGF-2 without exogenous EGF (Fig 3.10A and B). Thus, these data suggest that the effect of DLX2 on proliferation depends on EGFR signaling.

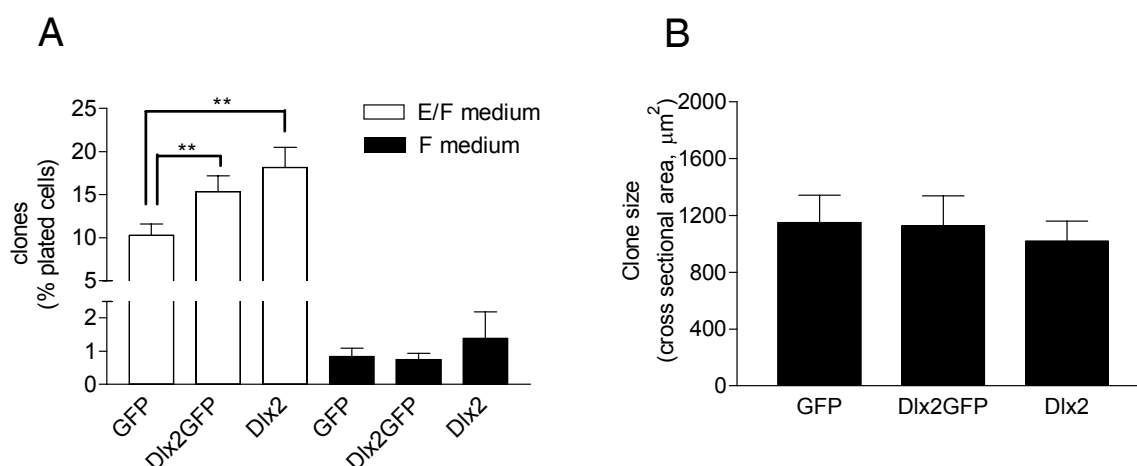


**Fig 3.10. Effect of DLX2 on proliferation depends on EGFR signaling**

Five days after infection and growth in E/F medium, transduced-cells were sorted to medium containing both EGF and FGF-2 or only FGF-2. Quantitative analysis of the percentage (A) and of the size (B) of clones revealed that in the absence of exogenous EGF, DLX2 over-expression had no effect on cell proliferation. Numbers represent the means  $\pm$  SEM of at least three independent experiments (\*\*,  $P < 0.01$ ).

### 3.4.2. DLX2 over-expression increases the number of EGFR<sup>high</sup> cells in cultures of aSVZ but not hippocampal NPCs

Since TAPs but not stem cells specifically require EGFR signaling to proliferate (Cesetti *et al* unpublished observation), the observation that DLX2 requires EGFR signaling to promote clone formation suggests that the extra number of clones observed upon over-expression of DLX2 in aSVZ is a consequence of an increase in the number of TAPs. Since EGFR<sup>high</sup> cells are mostly TAPs, I investigated whether DLX2 over-expression increases the number of EGFR<sup>high</sup> cells. To this end, after transduction, cells were grown in F medium for three days, and then the number of EGFR<sup>high</sup> cells was

quantified by FACS analysis. Indeed, this analysis revealed that *Dlx2*-transduced aSVZ cells had a higher percentage of EGFR<sup>high</sup> cells, compared to the GFP-transduced control (Fig 3.11A). In contrast, the percentage of EGFR<sup>high</sup> cells in hippocampal precursors was not increased but rather slightly decreased by DLX2 over-expression (Fig 3.11B).

Since DLX2 promoted cell proliferation (see Fig 3.6), the greater number of EGFR<sup>high</sup> cells observed upon over-expression of DLX2 in aSVZ cells could be a consequence of a general boost of cell proliferation in these cultures. However, this is unlikely because before the quantitative analysis of EGFR<sup>high</sup> cells, cell cultures had been kept in the presence of only FGF-2, a condition in which DLX2 over-expression has no effect on proliferation as shown before (see Fig 3.10). Furthermore, if the increase in the number of EGFR<sup>high</sup> cells upon DLX2 over-expression was due to higher proliferation rate, it should also be observed in hippocampal cultures whose proliferation rate is also promoted by DLX2 over-expression (see Fig 3.6B).

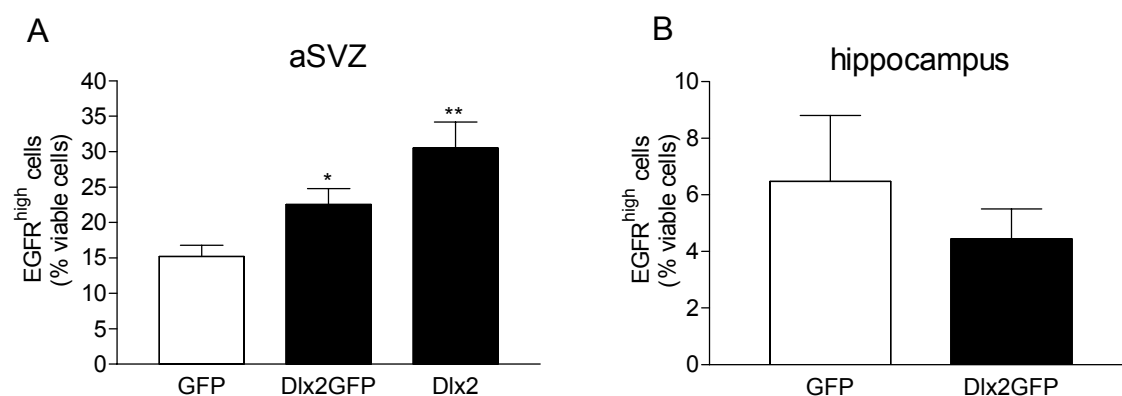


### Fig 3.11. Effect of DLX2 on the number of EGFR<sup>high</sup> cells

After tissue dissection and transduction with the indicated lentiviral constructs cells were cultured in medium containing only FGF-2 for three days. Thereafter, cells were stained with EGF-alexa647 and analyzed by FACS. Quantitative analysis of the number of EGFR<sup>high</sup> cells in aSVZ (A) and hippocampal (B) cultures transduced with the indicated lentiviral construct showing that Dlx2 over-expression increased the percentage of EGFR<sup>high</sup> cells only in aSVZ but not in hippocampal cultures. Numbers represent the means  $\pm$  SEM of at least three independent experiments (\*,  $P < 0.05$ ; \*\*,  $P < 0.01$ ).

### 3.4.3. DLX2 over-expression promotes the transition from EGFR<sup>low</sup> to EGFR<sup>high</sup> clone-forming cells in aSVZ but not hippocampal NPCs

Since the increase in the number of EGFR<sup>high</sup> cells observed in cultures of aSVZ precursors upon DLX2 expression is not likely due to increased proliferation rate of this cell population, I investigated whether it may be a consequence of a lineage transition of EGFR<sup>low</sup> primary neural stem cells to EGFR<sup>high</sup> TAPs (Morshead CM 1994; Ciccolini F 2001) by a process that in culture is promoted by exogenous FGF-2 (Ciccolini F 1998). I reasoned that in this case, over-expression of DLX2 should lead to a decrease of clone-

forming cells in the EGFR<sup>low</sup> cell population. To this end, dissociated aSVZ and hippocampal cells were transduced with the lentiviral constructs as previously described and then grown in F medium. Three days after transduction EGFR<sup>low</sup> cells were sorted by FACS and their clonogenic potential was analyzed by clonal analysis. As shown in Fig 3.12A, compared to GFP-transduced controls, the number of clone-forming cells was significantly lower in aSVZ EGFR<sup>low</sup> cells transduced with either DLX2 expressing lentiviral construct. Thus, both the increase in the number of EGFR<sup>high</sup> cells and the decrease in the number of clonogenic EGFR<sup>low</sup> cells observed upon over-expression of DLX2 in aSVZ NPCs suggest that in this population DLX2 promotes a lineage transition from EGFR<sup>low</sup> to EGFR<sup>high</sup> clone forming cells.

A similar analysis of hippocampal EGFR<sup>low</sup> cells revealed that the proportion of clone-forming cells in EGFR<sup>low</sup> cell population was not affected by DLX2 over-expression (Fig 3.12B). In addition, although EGFR<sup>low</sup> clone-forming cells were detected, their incidence was dramatically lower than the incidence of clonogenic NPCs in the population of aSVZ EGFR<sup>low</sup> cells (Fig 3.12C). Taken together, these results indicate that the DLX2 over-expression in aSVZ precursors leads to an expansion of EGFR<sup>high</sup> TAPs by promoting a lineage transition from EGFR<sup>low</sup> to EGFR<sup>high</sup> cells. Instead, over-expression of DLX2 did not lead to a similar cell lineage transition in hippocampal cells. Moreover, these data suggest that EGFR<sup>low</sup> precursors capable of becoming EGFR<sup>high</sup> cells are not present in the hippocampus or that their ability to up-regulate EGFR expression may be regulated by different mechanisms.

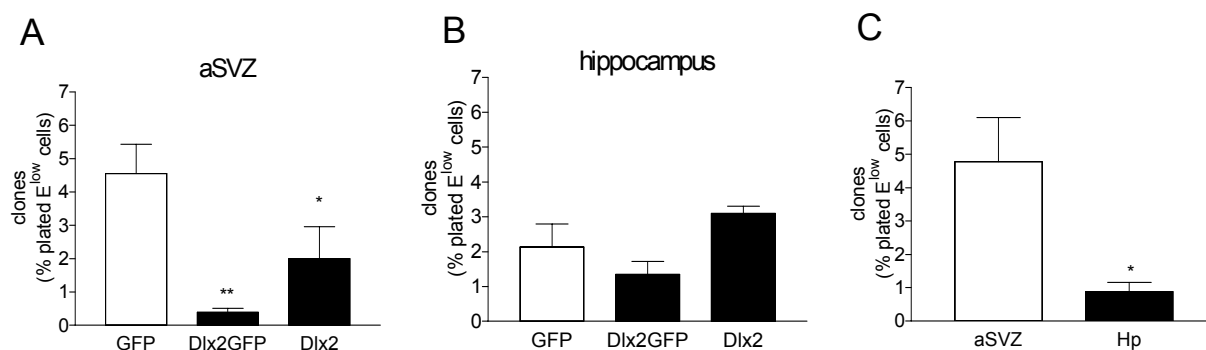


### Fig 3.12. Effect of DLX2 on cell lineage transition

(A-B) Quantitative analysis of the percentage of clones formed by EGFR<sup>low</sup> cells isolated by FACS from cultures of aSVZ and hippocampal cells that after dissociation and transduction with the indicated lentiviral constructs had been grown in FGF-2 containing medium for three days. Note that DLX2 over-expression decreases the number of clone-forming EGFR<sup>low</sup> cells in aSVZ (A) but not in hippocampal (B) cell cultures. (C) Quantitative analysis of the percentage of clones formed by EGFR<sup>low</sup> cells, which were sorted from dissociated aSVZ and hippocampal cells cultured overnight in FGF-2 containing medium after dissection. Numbers represent the means  $\pm$  SEM of at least three independent experiments (\*,  $P < 0.05$ ; \*\*,  $P < 0.01$ ).

#### 3.4.4. EGFR transcription is not regulated by DLX2

Since DLX2 is a homeodomain transcription factor, DLX2 could interact with *Egfr* promoter and upregulate *Egfr* expression leading to an increase in the number of EGFR<sup>high</sup> cells. To investigate this possibility, I transduced HEK293FT cells with a lentiviral construct, LV EGFRP GFP, kindly provided from miss K. Obernier, in which GFP is expressed under the control of the murine *Egfr* promoter and afterwards transfected them with a DLX2 expressing plasmid. Semi-quantitative RT-PCR analysis revealed that the level of GFP transcript was not regulated by DLX2 over-expression

(Fig 3.13A). In addition, qRT PCR analysis showed that DLX2 over-expression in aSVZ EGFR<sup>high</sup> cells did not lead to an increase of *Egfr* mRNA level (Fig 3.13B). Taken together, these data indicate that DLX2 does not directly regulate transcription/stability of *Egfr* mRNA.

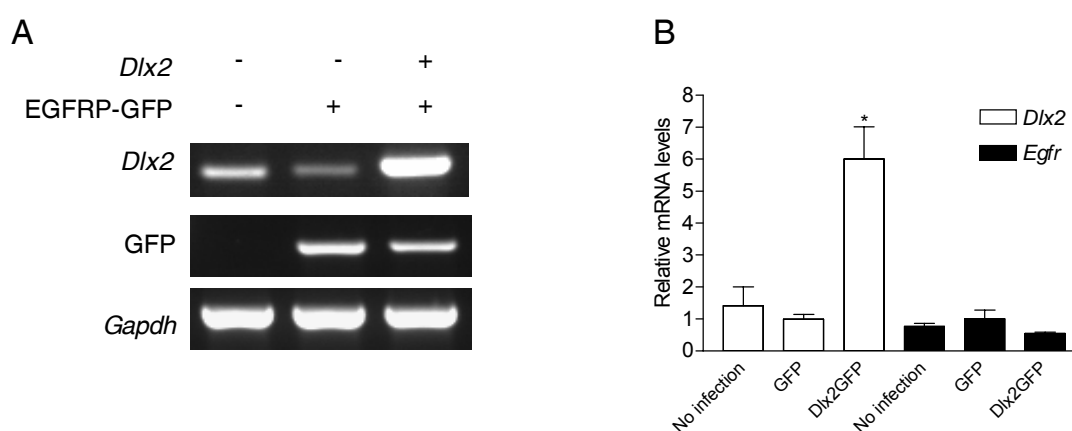


### Fig 3.13. DLX2 does not affect levels of EGFR mRNA

(A) HEK293FT cells were transfected by *Dlx2* expression vector and/or transduced by LV EGFRP GFP, in which GFP is expressed under the control of EGFR promoter. Levels of *Dlx2* and GFP were analyzed by semi-quantitative RT-PCR. The level of *Gapdh* mRNA was used for endogenous control. Note that GFP expression is not affected by over-expression of *Dlx2*. (B) EGFR<sup>high</sup> cells transduced by LV GFP or LV Dlx2GFP were sorted for RNA extraction after 4 days of transduction of aSVZ cells dissected from postnatal (P7) mice. Gene expression levels of *Dlx2* and *Egfr* were analyzed by qRT PCR and were normalized to the expression of endogenous gene, *beta-2 microglobulin* (*β2M*). Numbers represent the relative levels of mRNA, compared to one of GFP-transduced EGFR<sup>high</sup> cells. Note that though *Dlx2* expression was higher, *Egfr* expression was not increased in Dlx2GFP-transduced EGFR<sup>high</sup> cells.

## 4. Discussion

### 4.1. Hippocampal EGFR<sup>high</sup> cells display intrinsically different properties from aSVZ EGFR<sup>high</sup> cells

In this doctoral work, I have used direct isolation to compare the characteristics of clone-forming cells of the hippocampus and the aSVZ. Using this approach I was able to show that at least a portion of EGFR<sup>high</sup> cells in the hippocampus display characteristics of NPCs derived from the MGE, suggesting that hippocampal EGFR<sup>high</sup> cells have a ventral origin. I found that hippocampal EGFR<sup>high</sup> cells, like their counterpart in the GE, express *Nkx2.1*, the homeobox transcription factor. *Nkx2.1* is known to define the regional boundary of the medial GE (MGE). Transgenic mice lacking the expression of *Nkx2.1* showed abnormal development of the MGE with an apparent conversion of the MGE to an LGE-like phenotype (Sussel L 1999). In particular, the hippocampus of *Nkx2.1* mutant mice showed a decrease in the number of cells expressing DLX2 and GABAergic interneurons. It has been previously shown that MGE-derived cells expressing NKX2.1 and DLX2, migrate dorsally along tangential routes into the cortex and the hippocampus from early to late stages of embryonic development and give rise to GABAergic interneurons (Anderson SA 2001; Marin O 2001). Mice with mutation of both *Dlx1* and *Dlx2* display also defects in the development of the MGE and LGE (Anderson SA 1997; Marin O 2000). In addition, these mice showed almost a complete loss of GABAergic interneurons in the hippocampus, suggesting that many of tangentially migrating cells appear to require the function of the *Dlx2* homeobox gene. However, although DLX2 is required for the

development of hippocampal interneurons, it is likely that tangentially migrating cells down-regulate DLX2 expression while migrating to the hippocampus. Indeed, it was found that a population of *Dlx2*-expressing cells migrates tangentially from the GE to the hippocampus during embryonic development where they are mainly concentrated in the CA1 region, similar region to hSVZ and after migration to the hippocampus they are weakly DLX2 immunopositive (Nery S 2003). Consistent with these observations, my data showed that hippocampal EGFR<sup>high</sup> cells are localized in the hSVZ region. In addition, I also found that although *Nkx2.1* is similarly expressed in EGFR<sup>high</sup> cells derived from both the aSVZ and the hippocampus, the expression of *Dlx2* is dramatically down-regulated in the hippocampal population. Taken together, these observations suggest that hippocampal EGFR<sup>high</sup> cells may represent NPCs migrating from the GE to the hippocampus during embryonic development. This interpretation is further supported by previous observation from our laboratory showing that EGFR expressing cells in the embryonic cortical germinal zone display both radial and tangential orientation (Ciccolini F 2005). In particular, analysis of EGFR expressing cells in the hSVZ mainly displayed a tangential orientation and no radially oriented cells were observed in this region (Suh *et al.*, submitted).

Despite the similarities of their origin and enrichment in clone-forming cell population, hippocampal EGFR<sup>high</sup> cells seem to be intrinsically different from aSVZ EGFR<sup>high</sup> cells. Although hippocampal EGFR<sup>high</sup> cells expressed relatively higher levels of EGFR than the rest of hippocampal cells, their expression levels of *Egfr* were significantly lower, compared with GE EGFR<sup>high</sup> cells. Moreover, hippocampal EGFR<sup>high</sup> cells expressed drastically lower levels of *Dlx2*. Reflecting these differences, the two precursor groups displayed differential potential of proliferation. Hippocampal EGFR<sup>high</sup> cells in

postnatal mice were less clonogenic, formed smaller clones and were less self-renewing, than aSVZ EGFR<sup>high</sup> cells. Taken together, this doctoral work suggests that clonogenic EGFR<sup>high</sup> cells in the hSVZ originate from the GE; however, they are intrinsically different from aSVZ precursors in terms of their potential of proliferation and the pattern of gene expression.

#### **4.2. Relationship between precursors in the hSVZ and neurogenesis in the dentate gyrus**

It is well established that lifelong neurogenesis persists in the dentate gyrus, and precursors supporting this process have been identified in this region (Seri B 2001; Kempermann G 2004). However, neural progenitors isolated from the adult murine DGs have limited proliferative capacity, and do not display *in vitro* long term self-renewal and multipotency, which are distinctive stem cell characteristics (Seaberg RM 2002). Instead, self-renewing multipotent NPCs were isolated from the hSVZ although it was shown that they require BDNF to undergo neurogenesis (Bull ND 2005). Becq *et al* compared the properties of hSVZ and DG precursors in adult mouse brain *in vivo* and *in vitro* (Becq H 2005). They showed DG precursors scarcely respond to EGF and produce around 8 times less neurospheres than hSVZ precursors *in vitro*, supporting my observation that EGFR<sup>high</sup> cells are more concentrated around 8 times in the hSVZ than the DG. Taken together, these previous reports are in line with my observation that most clone-forming EGFR<sup>high</sup> cells are not localized in the DG, but in the hSVZ.

Given the large continuous turnover of hippocampal neurons in the DG, this raises a

fundamental question of the location of the precursors responsible for neurogenesis in the DG. However, the fact that DG cells do not form clones does not necessarily implicate that there are no neural stem cells in this region. It is possible that neural stem cells in the DG are intrinsically different from the neural stem cells in the aSVZ and they require different conditions to proliferate *in vitro*. In line with this hypothesis, Babu *et al* showed the existence of self-renewing multipotent neural precursors from micro-dissected DG by using optimized-culture conditions (Babu H 2007). Also, Bonaguidi *et al* suggested that high levels of bone morphogenetic protein (BMP) signaling occur in hippocampal but not aSVZ precursors *in vitro*, and blocking BMP signaling is sufficient to foster hippocampal cell self-renewal and multipotency. Therefore, DG stem cells may be intrinsically different from aSVZ stem cells, requiring different conditions for their expansion *in vitro*.

It is also conceivable that, at least in the neonatal brain, precursors in the hSVZ give rise to a subset of cells in the DG precursors. Injection of retrovirus encoding GFP in the neonatal hSVZ revealed that dividing precursors in this area give rise to cells that migrate to surrounding regions, including the DG (Navarro-Quiroga I 2006). They found that a subset of postnatal hSVZ cells are multipotent and express the precursor markers Sox2 and Musashi-1 and migrate into the DG giving rise to granule neurons and both radial and horizontal astrocytes in the DG, suggesting that postnatal hSVZ precursors contribute astrocyte-like neural stem cells to the adult stem cell niche in the SGZ of the hippocampal DG. More recently, it has also been found that cells migrating from the hSVZ to the DG are not homogenous as indicated by the expression of Neurogenin 2 and of Mash-1 (Kim EJ 2007; Galichet C 2008). Therefore, it will be important in the future to investigate the contribution of EGFR expressing cells to this

hSVZ/DG migratory stream observed in the neonatal hippocampus.

### **4.3. Differential effect of DLX2 in precursors of the aSVZ and the hippocampus**

DLX2 is an essential regulator of interneuron neurogenesis not only during embryonic development but also in the postnatal brain (Doetsch F 2002; Panganiban G 2002; Saino-Saito S 2003; Brill MS 2008). However, the mechanisms underlying the effect of DLX2 on neurogenesis are not clear. This doctoral work suggests that DLX2 promotes neurogenesis by selectively amplifying a pool of non-clonogenic precursors that upon differentiation give rise to GABAergic neurons. In this study, *Dlx2*-transduced cells derived from both the aSVZ and the hippocampus formed bigger size of clones, meaning that they proliferated more than the control counterpart. Since the effect of DLX2 on cell proliferation depended on EGFR signaling, DLX2 may have promoted the proliferation of EGFR expressing TAPs. However, although the extra proliferating cells found in DLX2 over-expressing clones responded to EGF, they were not self-renewing. This is consistent with the previous observations showing that blockade of DLX2 transcriptional activity *in vivo* decreases the number of fast proliferating aSVZ precursors leading to a decrease in neuroblasts (Brill MS 2008). However, Brill *et al* observed that over-expression of DLX2 *in vivo* promoted generation of more neuroblasts without affecting proliferation. Thus, they concluded that DLX2 affects directly the neuronal fate decision, while at the same time also being required for regulating precursor proliferation. One explanation of the discrepancy between *in vivo*

and *in vitro* would be that levels of EGFR signaling and DLX2 may determine the proliferative behavior of NPCs. It is possible that *in vivo*, in the absence of up-regulation of EGFR signaling, DLX2 over-expressing cells will not proliferate. Instead, in this situation, DLX2 may affect directly neuronal fate decision. In contrast, *in vitro*, EGFR signaling may not be a limiting factor anymore by exogenous EGF. Levels of DLX2 rather than EGFR signaling may limit proliferation *in vitro*, in which over-expression of DLX2 could promote proliferation. Therefore, by concomitantly up-regulating DLX2 and EGFR signaling *in vitro*, my work has underscored previously unknown mechanisms by which DLX2 affects neurogenesis.

Furthermore, this doctoral work suggests that DLX2 promotes cell lineage transition from slowly dividing quiescent stem cells to rapidly proliferating TAPs in aSVZ cells (Fig 4.1A). Previous analysis have shown that EGFR<sup>high</sup> TAPs are generated from clonogenic EGFR<sup>low</sup> precursors (Morshead CM 1994; Ciccolini F 2001). In this study, I show that over-expression of DLX2 in aSVZ precursors leads to an initial increase in the percentage of EGFR<sup>high</sup> cells (TAPs) and to a concomitant decrease in type B cells, EGFR<sup>low</sup> precursors. My data also reveal that this effect is not due to an extra proliferation of EGFR<sup>high</sup> cells or to a direct effect of DLX2 on EGFR expression. Rather, my data suggest that DLX2 may instructs or accelerates the cell lineage transition from EGFR<sup>low</sup> primitive stem cells to EGFR<sup>high</sup> clone forming cells (Ciccolini F 2001), resulting in the increase of EGFR<sup>high</sup> cells and more clone forming cells.

Although, as in the aSVZ, forced expression of DLX2 in hippocampal cells also promoted proliferation and neurogenesis, an increase in lineage transition from EGFR<sup>low</sup> to EGFR<sup>high</sup> cells was not observed in this cell group (Fig 4.1B). DLX2 over-expression in hippocampal cells neither increased the percentage of EGFR<sup>high</sup> cells (TAPs) nor

decreased quiescent stem cells so that DLX2 did not affect on the percentage of hippocampal clone-forming cells. The observations that DLX2 promote cell lineage transition only in aSVZ precursors but not in hippocampal precursors suggest that primitive EGFR<sup>low</sup> precursors being able to convert to EGFR<sup>high</sup> TAPs are not present in the hippocampus or that the lineage transition may be regulated by different mechanisms. The interpretation of this data is complicated by the fact that is not still clear whether aSVZ and hSVZ precursors are directly related. If the lineage transition is regulated by different mechanisms in the hippocampus, it would mean that hippocampal EGFR<sup>high</sup> cell population could be regulated locally by cell lineage transition. Instead, if the lineage transition does not occur, all hippocampal EGFR<sup>high</sup> cells may originate from the GE and the population would be decreased by postnatal migration or differentiation with aging. Thus, it remains to investigate whether there are resident EGFR<sup>low</sup> cells being able to convert to EGFR<sup>high</sup> cells in the hippocampus.

It was previously found that sustained EGF infusion in the lateral ventricle elicits neural stem cell activity in TAPs and causes a down-regulation of DLX2 expression in the aSVZ (Doetsch F 2002), suggesting that TAPs are not irreversibly committed to the generation of neuroblasts. Taken together, therefore, this doctoral work suggests that a cross talk between DLX2 and EGFR signaling is a key for the maintenance of cell homeostasis in the aSVZ.

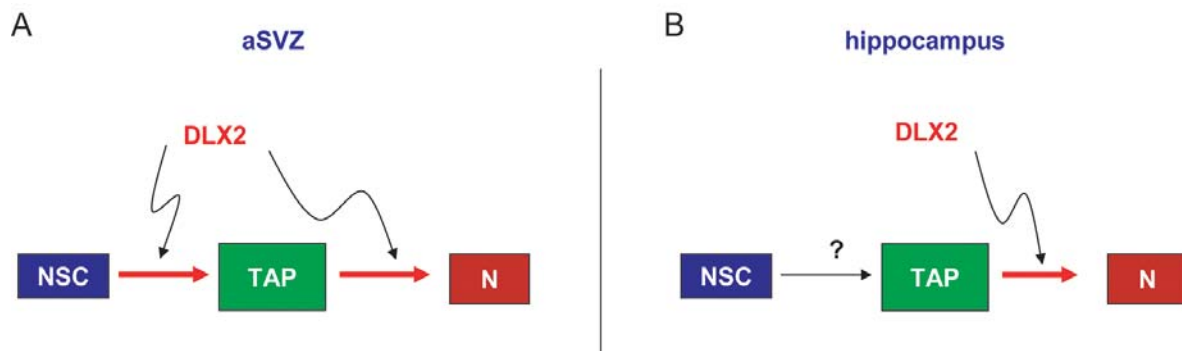


**Fig. 4.1. Schematic model of DLX2 effect in NPCs derived from the aSVZ and the hippocampus**

DLX2 over-expression has positive effect on generation of neurons in both aSVZ (A) and hippocampal NPC cultures (B), however it promotes cell lineage transition from NSC to TAP only when over-expressed in NPCs derived from the aSVZ (A) but not hippocampal cell culture (B). NSC, quiescent neural stem cell; TAP, transit-amplifying precursor; N, neuroblast.

## 5. Conclusions and prospects

To realize the potential of neural stem cell therapy, it is important to know their identity and the molecular mechanisms by which their proliferation/differentiation is regulated to maintain cell homeostasis. In this study, I characterized putative neural stem cells in the hippocampus and the aSVZ of postnatal mouse and investigated the function of DLX2 in NPCs. Similarly to the aSVZ, hippocampal clone-forming cells were localized

to the SVZ rather than neurogenic region, the DG in the hippocampus. Their expression of *Nkx2.1*, a regional marker of the MGE suggested that at least a subset of them originate from the GE during embryonic development. However, despite their similarity of origin, localization in the SVZ and enrichment in clone-forming cell population, the analysis of gene expression levels (*Egfr*, *Dlx2*) and clonal analysis revealed that they are intrinsically different each other. Since subsets of dividing precursors in the hSVZ are known to migrate to surrounding regions, including the DG (Navarro-Quiroga I 2006), it would be important in a future to study the contribution of EGFR expressing cells to this hSVZ/DG migratory stream observed in the neonatal hippocampus.

A study to modulate gene expression levels of DLX2 indicated that DLX2 increases proliferation rate and neuronal differentiation in NPCs derived from both the aSVZ and the hippocampus, depending on EGFR signaling. However, DLX2 promoted cell lineage progression from EGFR<sup>low</sup> quiescent stem cells to EGFR<sup>high</sup> TAPs only in aSVZ-derived NPCs but not in hippocampal NPCs, suggesting primitive EGFR<sup>low</sup> precursors being able to convert to EGFR<sup>high</sup> TAPs may not be present in the hippocampus or that the lineage transition may be regulated by different mechanisms. Thus, it remains to investigate whether there are resident EGFR<sup>low</sup> cells being able to convert to EGFR<sup>high</sup> cells in the hippocampus.

Taken together, this doctoral work suggests that hippocampal EGFR<sup>high</sup> cells are intrinsically different from aSVZ precursors with respect to their stem cell properties. Also, this study suggests that a cross talk between DLX2 and EGFR signaling is a key for the maintenance of cell homeostasis in the aSVZ. Thus, a further study to understand the mechanisms by which DLX2 promotes cell lineage transition may also provide important tools to modulate stem cell activity *in vivo*.

## 6. References

Alvarez-Buylla A (1990). "Proliferation "hot spots" in adult avian ventricular zone reveal radial cell division." *Neuron* **5**: 101-109.

Alvarez-Buylla A (2001). "A unified hypothesis on the lineage of neural stem cells." *Nat Rev Neurosci.* **2**: 287-293.

Alvarez-Buylla A (2004). "For the long run: maintaining germinal niches in the adult brain." *Neuron* **41**: 683-686.

Anderson SA (1997). "Interneuron migration from basal forebrain to neocortex: dependence on *Dlx* genes." *Science* **278**: 474-476.

Anderson SA (1997). "Mutations of the homeobox genes *Dlx-1* and *Dlx-2* disrupt the striatal subventricular zone and differentiation of late born striatal neurons." *Neuron* **19**: 27-37.

Anderson SA (2001). "Distinct cortical migrations from the medial and lateral ganglionic eminences." *Development* **128**: 353-363.

Babu H (2007). "Enriched monolayer precursor cell cultures from micro-dissected adult mouse dentate gyrus yield functional granule cell-like neurons." *PLoS ONE.* **2**(e388).

Becq H (2005). "Differential properties of dentate gyrus and CA1 neural precursors." *J Neurobiol.* **62**: 243-261.

Bernard P (1992). "Cell killing by the F plasmid *CcdB* protein involves poisoning of DNA-topoisomerase II complexes." *J Mol Biol.* **226**: 735-745.

Brill MS (2008). "A *dlx2*- and *pax6*-dependent transcriptional code for periglomerular neuron specification in the adult olfactory bulb." *J Neurosci.* **28**: 6439-6452.

Bull ND (2005). "The adult mouse hippocampal progenitor is neurogenic but not a stem cell." *J. Neurosci.* **25**: 10815-10821.

- Bushman W (1985). "Control of directionality in lambda site specific recombination." *Science* **230**: 906-911.
- Cameron HA (1993). "Differentiation of newly born neurons and glia in the dentate gyrus of the adult rat." *Neuroscience* **56**: 337-344.
- Ciccolini F (1998). "Fibroblast growth factor 2 (FGF-2) promotes acquisition of epidermal growth factor (EGF) responsiveness in mouse striatal precursor cells: identification of neural precursors responding to both EGF and FGF-2." *J Neurosci.* **18**: 7869-7880.
- Ciccolini F (2001). "Identification of two distinct types of multipotent neural precursors that appear sequentially during CNS development." *Mol Cell Neurosci.* **17**: 895-907.
- Ciccolini F (2005). "Prospective isolation of late development multipotent precursors whose migration is promoted by EGFR." *Dev. Biol* **284**: 112-125.
- Corbin JG (2000). "The Gsh2 homeodomain gene controls multiple aspects of telencephalic development." *Development* **127**: 5007-50020.
- Corbin JG (2001). "Telencephalic cells take a tangent: non-radial migration in the mammalian forebrain." *Nat Neurosci.* **4**: 1177-1182.
- de Carlos JA (1996). "Dynamics of cell migration from the lateral ganglionic eminence in the rat." *J Neurosci.* **16**: 6146-6156.
- Doetsch F (1997). "Cellular composition and three-dimensional organization of the subventricular germinal zone in the adult mammalian brain." *J Neurosci.* **17**: 5046-5061.
- Doetsch F (2002). "EGF converts transit-amplifying neurogenic precursors in the adult brain into multipotent stem cells." *Neuron* **36**: 1021-1034.
- Eisenstat DD (1999). "DLX-1, DLX-2, and DLX-5 expression define distinct stages of basal forebrain differentiation." *J. Com. Neurol.* **414**: 217-237.

- Filippov V (2003). "Subpopulation of nestin-expressing progenitor cells in the adult murine hippocampus shows electrophysiological and morphological characteristics of astrocytes." *Mol Cell Neurosci.* **23**: 373-382.
- Fukuda S (2003). "Two distinct subpopulations of nestin-positive cells in adult mouse dentate gyrus." *J Neurosci.* **23**: 9357-9366.
- Gage FH (2000). "Mammalian neural stem cells." *Science* **287**: 1433-1438.
- Galichet C (2008). "Neurogenin 2 has an essential role in development of the dentate gyrus." *Development* **135**: 2031-2041.
- Garcia-Verdugo JM (2002). "The proliferative ventricular zone in adult vertebrates: a comparative study using reptiles, birds, and mammals." *Brain Res Bull.* **57**: 765-775.
- Graham FL (1977). "Characteristics of a human cell line transformed by DNA from human adenovirus type 5." *J Gen Virol.* **36**: 59-74.
- Guillemot F (2005). "Cellular and molecular control of neurogenesis in the mammalian telencephalon." *Curr Opin Cell Biol.* **17**: 639-647.
- Harrison T (1977). "Host-range mutants of adenovirus type 5 defective for growth in HeLa cells." *Virology* **77**: 319-329.
- Himeno (1984). "Effect of polyethylene glycol in plasmid DNA on transformation of CaCl<sub>2</sub>- treated Escherichia coli cells." *Agric. Biol. Chem.* **48**: 657-662.
- Ihrig RA (2008). "Cells in the astroglial lineage are neural stem cells." *Cell Tissue Res.* **331**: 179-191.
- Kempermann G (2004). "Milestones of neuronal development in the adult hippocampus." *Trends Neurosci.* **27**: 447-452.
- Kim EJ (2007). "In vivo analysis of Ascl1 defined progenitors reveals distinct developmental dynamics during adult neurogenesis and gliogenesis." *J Neurosci.* **27**: 12764-12774.

- Liu JK (1997). "Dlx genes encode DNA-binding proteins that are expressed in an overlapping and sequential pattern during basal ganglia differentiation." *Dev Dyn* **210**: 498-512.
- Lois C (2002). "Germline transmission and tissue-specific expression of transgenes delivered by lentiviral vectors." *Science* **295**: 868-872.
- Malatesta P (2000). "Isolation of radial glial cells by fluorescent-activated cell sorting reveals a neuronal lineage." *Development* **127**: 5253-5263.
- Malatesta P (2008). "Radial glia and neural stem cells." *Cell Tissue Res.* **331**: 165-178.
- Marin O (2000). "Origin and molecular specification of striatal interneurons." *2000* **20**: 6063-6076.
- Marin O (2001). "A long, remarkable journey: tangential migration in the telencephalon." *Nat Rev Neurosci.* **2**: 780-790.
- McGuinness T (1996). "Sequence, organization, and transcription of the Dlx-1 and Dlx-2 locus." *Genomics* **35**: 473-485.
- Menezes JR (1994). "Expression of neuron-specific tubulin defines a novel population in the proliferative layers of the developing telencephalon." *J. Neurosci.* **14**: 5399-5416.
- Mercier F (2002). "Anatomy of the brain neurogenic zones revisited: fractones and the fibroblast/macrophage network." *J Comp Neurol.* **451**: 170-188.
- Merkle FT (2004). "Radial glia give rise to adult neural stem cells in the subventricular zone." *Proc Natl Acad Sci U S A.* **101**: 17528-17532.
- Merkle FT (2006). "Neural stem cells in mammalian development." *Curr Opin Cell Biol.* **18**: 704-709.
- Morshead CM (1994). "Neural stem cells in the adult mammalian forebrain: a relatively quiescent subpopulation of subependymal cells." *Neuron* **13**: 1071-1082.

Naldini L (1996). "In vivo gene delivery and stable transduction of nondividing cells by a lentiviral vector." *Science* **272**: 263-267.

Navarro-Quiroga I (2006). "Postnatal cellular contributions of the hippocampus subventricular zone to the dentate gyrus, corpus callosum, fimbria, and cerebral cortex." *J. Com. Neurol.* **497**: 833-845.

Nery S (2003). "Dlx2 progenitor migration in wild type and Nkx2.1 mutant telencephalon." *Cereb. Cortex* **13**: 895-903.

Oh-hora M (2003). "Requirement for Ras guanine nucleotide releasing protein 3 in coupling phospholipase C-gamma2 to Ras in B cell receptor signaling." *J Exp Med.* **198**: 1841-1851.

Panganiban G (2002). "Developmental functions of the Distal-less/Dlx homeobox genes." *Development* **129**: 4371-4386.

Pleasure SJ (2000). "Cell migration from the ganglionic eminences is required for the development of hippocampal GABAergic interneurons." *Neuron* **28**: 727-740.

Ptashne M (1992). "Genetic Switch: Phage Lambda and Higher Organisms." *Cambridge, MA: Cell Press*.

Qiu M (1995). "Null mutation of Dlx-2 results in abnormal morphogenesis of proximal first and second branchial arch derivatives and abnormal differentiation in the forebrain." *Genes Dev.* **9**: 2523-2538.

Rubenstein JL (1994). "The embryonic vertebrate forebrain: the prosomeric model." *Science* **266**: 578-580.

Russo RE (2004). "Functional and molecular clues reveal precursor-like cells and immature neurones in the turtle spinal cord." *J Physiol.* **560**: 831-838.

Saino-Saito S (2003). "Dlx-1 and Dlx-2 expression in the adult mouse brain: relationship to dopaminergic phenotypic regulation." *J. Com. Neurol.* **461**: 18-30.

- Seaberg RM (2002). "Adult Rodent Neurogenic Regions: The Ventricular Subependyma Contains Neural Stem Cells, But the Dentate Gyrus Contains Restricted Progenitors." *J. Neurosci.* **22**: 1784-1793.
- Seri B (2001). "Astrocytes give rise to new neurons in the adult mammalian hippocampus." *J. Neurosci.* **21**: 7153-7160.
- Steiner B (2006). "Type-2 cells as link between glial and neuronal lineage in adult hippocampal neurogenesis." *Glia* **54**: 805-814.
- Stoykova A (2000). "Pax6 modulates the dorsoventral patterning of the mammalian telencephalon." *J Neurosci.* **20**: 8042-8050.
- Sussel L (1999). "Loss of Nkx2.1 homeobox gene function results in a ventral to dorsal molecular respecification within the basal telencephalon: evidence for a transformation of the pallidum into the striatum." *Development* **126**: 3359-3370.
- Temple S (1999). "Stem cells in the adult mammalian central nervous system." *Curr Opin Neurobiol.* **9**: 135-141.
- Toresson H (2000). "Genetic control of dorsal-ventral identity in the telencephalon: opposing roles for Pax6 and Gsh2." *Development* **127**: 4361-4371.
- Wichterle H (1999). "Young neurons from medial ganglionic eminence disperse in adult and embryonic brain." *Nat Neurosci.* **2**: 461-466.
- Yun K (2001). "Gsh2 and Pax6 play complementary roles in dorsoventral patterning of the mammalian telencephalon." *Development* **128**: 193-205.
- Zhou QP (2004). "Identification of a direct Dlx homeodomain target in the developing mouse forebrain and retina by optimization of chromatin immunoprecipitation." *Nucleic Acids Res.* **32**: 884-892.
- Zufferey R (1997). "Multiply attenuated lentiviral vector achieves efficient gene delivery in vivo." *Nat Biotechnol.* **15**: 871-875.

Zupanc GK (2006). "Neurogenesis and neuronal regeneration in the adult fish brain." *J Comp Physiol A Neuroethol Sens Neural Behav Physiol.* **192**: 649-670.

## 7. Abbreviations

AEP	anterior entopeduncular area
Amp	Ampicillin
aSVZ	anterior SVZ
bp	base pair
CA1	<i>Cornu Ammonis</i> area 1
cDNA	complementary DNA
CNS	central nervous system
Dlx	dista-less homeobox gene
DG	dentate gyrus
DMSO	Dimethyl sulfoxide
DNA	Deoxyribonucleic acid
dNTP	Deoxyribonucleoside triphosphate
DTT	Dithiothreitol
<i>E. coli</i>	<i>Escherichia coli</i>
EDTA	Ethylene-diamine-tetraacetic acid
EGF	epidermal growth factor
EGFR	epidermal growth factor receptor
FACS	fluorescent-activated cell sorting
FCS	fetal calf serum
FGF-2	fibroblast growth factor-2
Fig	Figure
GABA	gamma-aminobutyric acid
GAPDH	Glyceraldehyde-3-phosphate dehydrogenase
GE	ganglionic eminence
GFAP	glial fibrillary associated protein
GFP	green fluorescence protein
HP	hippocampus
hSVZ	hippocampal SVZ
kb	kilo base pair
kDa	kilodaltons
LB	Luria-Bertani
LGE	lateral ganglionic eminence
LV	lentivirus

MGE	medial ganglionic eminence
mRNA	messenger RNA
NKX2.1	NK2 homeobox 1
NPCs	neural stem/precursor cells
Pax6	paired box 6 gene
PBS	phosphate buffered saline
PCR	polymerase chain reaction
PI	propidium iodide
qRT PCR	quantitative RT PCR
RNA	Ribonucleic acid
RT PCR	reverse transcription PCR
SDS	Sodium dodecyl sulfate
SDS-PAGE	SDS polyacrylamide gel electrophoresis
SGZ	subgranular zone
SVZ	subventricular zone
TAPs	transit-amplifying precursors

### 8. Acknowledgements

This is perhaps the easiest and hardest part that I have to write. It will be simple to name all the people that helped to get this done, but it will be tough to thank them enough. First of all, I would like to express sincere appreciation to my advisor, Dr. Francesca Ciccolini for her great support and thoughtful guidance for this study. I also thank to all group members. It would be impossible to finish this thesis without their helps. Especially, I express deeply-felt thanks to Gaby Hölzl-Wenig, Alexia Herrmann and Ms. Kirsten Obernier who helped me to finish this study.

I am also thankful to Dr. Pavel Osten and Oh-hora M. who had provided me cell line and plasmids for lentiviral production. Also I express many thanks to Prof. Dr. Hilmar Bading and Prof. Dr. Gabriele Elisabeth Pollerberg for supervising this dissertation. I also thank the members of my thesis committee: Prof. Dr. Christoph Schuster and Prof. Dr. Ulrike Müller. I can not forget to thank to the Landesstiftung for their generous funding.

I deeply express my gratitude to my wife, Mishil Kim for her love and encouragement and emotional support that made me survive in Germany. I am also thankful to my mother and sisters for their endless love. Also, I would like to give thanks to Pastor In-Chan Yeon and all members of my church for their heartfelt prayer.

Above all, I thank to God.